Radboud Repository

Radboud University Nijmegen

PDF hosted at the Radboud Repository of the Radboud University Nijmegen

The following full text is a publisher's version.

For additional information about this publication click this link.
http://hdl.handle.net/2066/22801

Please be advised that this information was generated on 2017-12-05 and may be subject to change.

THE JOURNAL OF COMPARATIVE NEUROLOGY 375:18–42 (1996)

Projection Neurons of the Mormyrid Electrosensory Lateral Line Lobe: Morphology, Immunohistochemistry, and Synaptology

K. GRANT, J. MEEK, Y. SUGAWARA, M. VERON, J.P. DENIZOT, T.G.M. HAFMANS, J. SERRIER, AND T. SZABO†
CNRS, Institut Alfred Fessard, 91190 Gif-sur-Yvette, France (K.G., Y.S., M.V., J.P.D., J.S., T.S.); Department of Anatomy and Embryology, University of Nijmegen, 6500 HB Nijmegen, The Netherlands (J.M., T.G.M.H.)

ABSTRACT

This paper describes the morphological, immunohistochemical, and synaptic properties of projection neurons in the highly laminated medial and dorsolateral zones of the mormyrid electrosensory lateral line lobe (ELL). These structures are involved in active electrolocation, i.e., the detection and localization of objects in the nearby environment of the fish on the basis of changes in the reafferent electrosensory signal generated by the animal's own electric organ discharge. Electrosensory, corollary electromotor command-associated signals (corollary discharges), and a variety of other inputs are integrated within the ELL microcircuit. The organization of ELL projection neurons is analyzed at the light and electron microscopic levels based on Golgi impregnations, intracellular labeling, neuroanatomical tracer techniques, and γ-aminobutyric acid (GABA), γ-aminobutyric acid decarboxylase (GAD), and glutamate immunohistochemistry.

Two main types of ELL projection neurons have been distinguished in mormyrids: large ganglionic (LG) and large fusiform (LF) cells. LG cells have a multipolar cell body (average diameter 13 μm) in the ganglionic layer, whereas LF cells have a fusiform cell body (on average, about 10 × 20 μm) in the granular layer. Apart from the location and shape of their soma, the morphological properties of these cell types are largely similar. They are glutamatergic and project to the midbrain torus semicircularis, where their axon terminals make axodendritic synaptic contacts in the lateral nucleus. They have 6–12 apical dendrites in the molecular layer, with about 10,000 spines contacted by GABA-negative terminals and about 3,000 GABA-positive contacts on the smooth dendritic surface between the spines. Their somata and short, smooth basal dendrites, which arborize in the plexiform layer (LG cells) or in the granular layer (LF cells), are densely covered with GABA-positive, inhibitory terminals.

Correlation with physiological data suggests that LG cells are I units, which are inhibited by stimulation of the center of their receptive fields, and LF cells are E units, excited by electric stimulation of the receptive field center. Comparison with the projection neurons of the ELL of gymnotiform fish, which constitute another group of active electrolocating teleosts, shows some striking differences, emphasizing the independent development of the ELL in both groups of teleosts. © 1996 Wiley-Liss, Inc.

Indexing terms: γ-aminobutyric acid, glutamate, Golgi impregnation, intracellular labeling, teleost

Actively electric African mormyrid fish have an electric organ that is situated at the base of the tail with a pulse-type discharge that generates an instantaneous electric field around the fish. This stimulates three types of cutaneous electroreceptors: knollenorgans, which are involved in intraspecific communication; mormyromasts, which are used for active electric imaging of the environment; and ampullary organs, which provide a passive electric sense. A similar active electric system serves compa-

Accepted May 30, 1996.

Y. Sugawara is currently at the Department of Physiology, Teikyo University School of Medicine, KAGA 2-11-1, Itabashi-ku, Tokyo 173, Japan.

Address reprint requests to J. Meek, Department of Anatomy and Embryology, University of Nijmegen, P.O. Box 9101, 6500 HB Nijmegen, The Netherlands. E-mail: J.meek@anat.kun.nl

†Deceased November 28, 1993.

© 1996 WILEY-LISS, INC.

rable functions in the separately evolved gymnotid electric fish of South and Central America. A passive electric sense, which is mediated by ampullary electroreceptors and is sensitive to the low-frequency electrical fields present in the aquatic environment, is also found in several other teleost species that, themselves, are not electric, including catfish and African knifefish (for reviews, see Bass, 1986; Bell, 1986; Zakon, 1986).

Primary afferent fibers running in the lateral line nerves convey electrosensory input from the receptors to the rhombencephalic electrosensory lateral line lobe (ELL). The ELL of mormyrids consists of a highly laminated cortex that is divided bilaterally into three zones (Maler, 1973; Bell and Szabo, 1986) that correspond to the termination sites of the different receptor afferents. Primary afferents innervating mormyromast type A and type B receptor cells terminate in the mediodorsal zone (MZ) and dorsolateral zone (DLZ) regions, respectively (Bell et al., 1989; Bell, 1990a,b), and primary afferents innervating ampullary receptors terminate in the ventrolateral zone (VLZ) region (Bell and Russell, 1978); a separate nucleus that is present bilaterally receives input from knollenorgan receptors (Enger et al., 1976; Bell and Russell, 1978; Szabo et al., 1983; Denizot et al., 1987; Mugnaini and Maler, 1987). The primary afferent projections to all three cortical zones of the ELL are topographically organized; thus, they generate three different images of the environment within this structure (Maler et al., 1973a,b; Bell and Russell, 1978). Inter- and intrazonal projections connect the different mormyromast zones (Bell et al., 1981).

Within the ELL, incoming electrosensory information is compared with an "expected" pattern that is encoded by an electric organ corollary discharge signal derived from the electromotor command nucleus and with central feedback from higher electrosensory processing centers (Bell et al., 1983; Bell and Szabo, 1986). Electrophysiological studies have shown that corollary discharge feedback to the electrosensory lobe operates as an active filter, which gates sensory processing in a context-related manner to distinguish between self-generated (reafferent) or extraneous (exafferent) electrosensory signals (Bell, 1986, 1989; Bell and Grant, 1989). In the mormyromast zones of the ELL, reafferent electric signals essential to active electrolocation are enhanced by a variety of complex and plastic interactions between electrosensory and electromotor command-associated inputs (Bell and Grant, 1992; Bell, 1993; Bell et al., 1993; Meek and Grant, 1994).

To understand fully the cellular mechanisms involved in the central gating of incoming sensory signals, a complete knowledge of the cytoarchitecture of the neuronal network of the ELL is essential. Although several studies have described the laminar organization of the mormyrid ELL cortex (Maler, 1973; Bell and Russell, 1978; Bell et al., 1981), and a Golgi study (Maler, 1973) has given a partial description of neuronal morphologies, the intrinsic organization of the sensory processing network is still largely unknown. In this paper, we present a description of the morphology and synaptic connections of the efferent neurons of the ELL that project via the lateral lemniscus to the preeminential nucleus in the isthmic region and to the lateral nucleus of the torus semicircularis in the midbrain (Bell et al., 1981). The results were obtained from light and electron microscope studies by using Golgi impregnation, anterograde and retrograde tracer labeling, immunohistochemistry, and intracellular labeling. The accompanying paper describes interneurons of the superficial layers of ELL (Meek et al., 1996), and a study of the deeper layers is in progress. Some preliminary results have been presented elsewhere (Meek, 1993, 1994; Meek and Grant, 1994).

Thorough investigations have already been made of the ELL and higher centers of some gymnotid electric fish with electric organ discharges that have a wave-type pattern (Maler, 1979; Bastian, 1981a,b; Maler et al., 1981, 1982; Carr et al., 1982; Heiligenberg and Dye, 1982; Bastian, 1986a,b; Mathieson et al., 1987; Bastian and Courtright, 1991; Bastian et al., 1993; Maler and Mugnaini, 1994). Because African mormyrids and American gymnotids developed active electrosensory systems independently during evolution (Bullock et al., 1982, 1983), comparison of the two groups may reveal the constraints and the possible variations in the evolution of these homologous structures. For this purpose, the present discussion makes a close comparison of the intrinsic structure of the mormyrid electrosensory lobe with that of the gymnotid. The sensory structures of passive electrosensory teleosts and the mechanosensory lateral line system, from which the electrosensory system evolved (McCormick, 1982, 1983), are also considered.

MATERIALS AND METHODS

Animals and surgery

The experiments described below were carried out by using a total of 63 fish of the species *Gnathonemus petersii*, which were obtained from registered fish dealers in Germany and The Netherlands. The fish ranged in length from 10 to 15 cm and were probably at the young adult stage. For the application of neuroanatomical tracers, surgery was carried out under anesthesia induced either with MS 222 (Sandoz: 35 mg/liter) or with Hypnodil (Janssen Lebrun: 4 mg/liter) added to the aquarium water. To avoid respiratory depression and to maintain a constant level of surgical narcosis, anesthetic solution was delivered through a tube inserted in the mouth and across the gills at a perfusion rate of 30 ml/minute. At the end of surgery, anesthetic solution was replaced with fresh aerated water. Recovery was calm, and the fish regained postural equilibrium and swam normally within 10–20 minutes. Before in vitro slice preparation or perfusion with fixatives in preparation for histology, fish were deeply anesthetized with MS 222 (65 mg/liter).

Neuroanatomical tracing techniques

Horseradish peroxidase (HRP). Projection neurons of the ELL were labelled by retrograde transport of HRP from their axon terminals in the lateral nucleus of the torus semicircularis. By using a surgical approach through the orbit under MS 222 anesthesia, the tip of a glass electrode covered with recrystallized HRP (made from a 10% solution in distilled H_2O evaporated at 4°C) was inserted into the lateral nucleus and left in place for 2 minutes. The wound was closed, and the fish recovered. After 3 days, the fish were reanesthetized deeply with MS 222 and perfused via the heart with 50 ml teleost ringer (Wolf, 1963) followed by 150 ml fixative containing 2% formaldehyde and 2% glutaraldehyde in 0.1 M phosphate buffer (PB), pH 7.4. The brain was removed and stored in the same fixative at 4°C overnight. Sixty-micron-thick sections of the ELL were cut on an Oxford Vibratome. Labeling was visualized by using the 3,5-diaminobenzidine (DAB) technique without intensification. Sections were mounted on glass slides, dehydrated, counterstained with cresyl violet, and mounted in DPX.

To label the terminal fields of electrosensory primary afferent fibers in the electrosensory lobe, the posterior lateral line nerve was cut close to its exit from the skull, below the base of the otic capsule, and recrystallized HRP was applied to the central stump. The fish were perfused 3 days later and were prepared for histology as above.

Phaseolus vulgaris-leucoagglutinin (PHA-L). Anterograde labeling of efferent pathways of the ELL was obtained following iontophoretic deposit of PHA-L in the electrosensory lobe. A small hole was drilled in the skull to expose the valvula above the electrosensory lobe. Injection sites were guided by the form of electrophysiologically recorded extracellular field potentials. These were evoked either by the corollary discharge signal arising from the electric organ central command nucleus or in response to reafferent or exafferent electrosensory input (see Bell et al., 1992). Field potentials were explored by using glass microelectrodes filled with 3 M NaCl (tip diameter 1.5 μm, resistance 3–5 MΩ). For iontophoretic deposit of PHA-L, fiber-containing glass electrodes were broken to give a tip diameter of 10–25 μm and were filled by capillarity with a 5% solution of PHA-L (Vector Laboratories, batch no. B0216) in 10 mM sodium phosphate-buffered saline (PBS), pH 8. Electrode tip resistances were 2–10 MΩ, and iontophoretic deposit of PHA-L was obtained by passing 5 μA current pulses (electrode tip positive) with a regime of 7 seconds on/ 7 seconds off for 10 minutes (Gerfen and Sawchenko, 1984). After a postinjection survival period of 5–10 days, the fish were reanesthetized and perfused for histology with 20 ml teleost ringer followed by 2% paraformaldehyde and 2% glutaraldehyde in 100 mM PB, as above.

After perfusion, the brain was removed, immersed for 3 hours in the same fixation fluid, and serial 100-μm-thick sections were cut in the transverse plane using a Vibratome. Alternate sections were treated for light microscopy (LM) and for electron microscopy (EM). For LM, sections were rinsed three times for 20 minutes in Tris-buffered saline (TBS), pH 7.35, preincubated in 0.1% bovine serum albumin (BSA) in TBS with 0.1% Triton X-100, and incubated overnight at room temperature in a biotinylated anti-PHA-L solution diluted 1:2,000 in preincubation medium. The sections were rinsed three times for 20 minutes in TBS, transferred for 60 minutes to a solution containing avidin-biotin complex (ABC) and 0.1% BSA in TBS, followed by three 20 minute rinses in TBS. Next, the sections were preincubated for 10 minutes in a solution containing 20 mg DAB and 300 mg nickel-ammonium sulphate per 100 ml of 0.05 M Tris, pH 7.6, followed by incubation for 5–10 minutes in the same solution after addition of 10 μl 30% H_2O_2. After two rinses in PBS, sections were dehydrated, some were counterstained with neutral red, and all were mounted in Entellan.

For EM, sections were treated similarly, but without Triton X-100 and nickel intensification. Instead, the DAB deposit was intensified by using the gold-substituted silver peroxidase (GSSP) method (van den Pol and Gorcs, 1986). For this purpose, sections were rinsed twice for 20 minutes in 2% sodium acetate and bleached for 3-4 hours in 10% thioglycolic acid. After four 20 minute rinses in sodium acetate, sections were developed for a maximum of 8 minutes in a mixture containing 10 ml of solution A (5% sodium carbonate), 10 ml of solution B (0.5 g silver nitrate, 0.5 g ammonium nitrate, and 2.5 g tungstosilic acid in 250 ml distilled water), and 40 μl of solution C (37% formaldehyde in water). Development was stopped by immersion for 2 minutes in 1% acetic acid. After three 20 minute rinses, the silver precipitate was substituted by gold during incubation for 8 minutes in 0.05% chloroauric acid ($H_4AuCl_4.xH_2O$; BDH Chemicals). After two 20 minute rinses in sodium acetate, sections were dehydrated in a graded series of ethanol and propylene oxide and were embedded in Epon between a slide and coverslip that were coated with Repelcoat, thus allowing the easy removal of selected sections at a later stage. Selected 100 μm sections were remounted on prepolymerized Epon blocks, and 80 nm ultrathin sections were cut by using a Reichert Ultracut-E. These sections were contrasted with uranyl acetate and lead citrate and were studied in a Philips EM 301.

Intracellular labeling

Intracellular labeling with Biocytin was carried out during electrophysiological recording with sharp electrodes in in vitro 400-μm-thick slice preparations of the ELL that were superfused in an interface-type chamber at room temperature (23–25°C) with artificial cerebrospinal fluid (ACSF) containing 124 mM NaCl, 2 mM KCl, 1.25 mM KH_2PO_4, 24 mM $NaHCO_3$, 2.6 mM $CaCl_2$, 1.6 mM $MgSO_4.7H_2O$, and 10 mM glucose, pH 7.3, after bubbling with 95% O_2/5% CO_2. Recording electrodes (tip diameters < 0.5 μm; resistance 150–200 MΩ) were filled with 2 or 4% Biocytin (Sigma) dissolved in 1.5 M potassium methyl sulfate. Hyperpolarizing DC currents of 0.5 nA applied for 5 minutes or more produced Golgi-like labeling of the recorded neurons (Horikawa and Armstrong, 1988). Slices were fixed overnight 1–6 hours after recording in 4% paraformaldehyde or in a mixture of 2% paraformaldehyde and 2% glutaraldehyde dissolved in 0.1 M PB, pH 7.4. After several washes in PB, the slices were treated in ethanol (50% for 20 minutes, 70% for 30 minutes, 50% for 20 minutes) to eliminate endogenous peroxidase activity (Metz et al., 1989), washed again in PB, and incubated in ABC complex (Vector standard ABC kit) for 1-2 hours using the technique supplied by the manufacturer. After three more washes in PB or PBS and then in Tris buffer, the slices were treated for 20–60 minutes with DAB dissolved in either 0.1 M PB or 0.05 M Tris buffer, pH 7.4, in the presence of cobalt chloride and nickel-ammonium sulphate to visualize biocytin labeling. Slices were rinsed well in buffer, counterstained while floating free in a drop of nuclear fast red (Merck), dehydrated while held flat beneath a coverslip, cleared in xylene, and mounted between two glass coverslips, which allowed the wholemount (nominally 400 μm before fixation and dehydration) to be viewed from either side.

Visualization of biocytin labeling was monitored periodically under a light microscope during development. Penetration of the reactifs was sufficient to give uniform labeling of intracellularly stained processes throughout the thickness of the slice after 20–60 minutes.

Golgi impregnation

Following perfusion and prefixation with aldehydes, the Golgi-rapid procedure was applied, including 3 days immersion of tissue at room temperature in a mixture of 0.2% osmium tetroxide and 2% potassium dichromate in distilled water followed by 2 days of immersion at room temperature in 0.75% silver nitrate. Serial sections, 50–100 μm thick, were cut in the transverse or sagittal plane on a Vibratome into the trough filled with 50% ethanol saturated with silver chromate (0°C; see Blackstad, 1975; Meek, 1981). The sections that were obtained were dehydrated with alcohol and xylene and mounted in DePeX. LM analysis was

performed by using a Leitz light microscope with a drawing tube.

Immunohistochemistry

For glutamate and γ-aminobutyric acid decarboxylase (GAD) immunohistochemistry, fish were deeply anesthetized with MS 222 and perfused with 20 ml teleost ringer followed by 150 ml 2% glutaraldehyde dissolved in 0.1 M PB, pH 7.2. The brain was removed and kept overnight in the same fixative at 4°C. After three washes (1 hour each) in 0.1 M PB, the brains were sectioned at 50 μm in an Oxford Vibratome.

Glutamate immunohistochemistry. Sections were treated in a solution of 1% sodium borohydride dissolved in 0.1 M PB, pH 7.2, for 1 hour. After three washes for 15 minutes in PB, the sections were incubated for 1 hour in 20% pig serum diluted in PBS (9 g NaCl/liter). This was followed by a wash in PBS containing 1% normal pig serum and by two further washes in PBS without normal pig serum. The sections were then incubated overnight in monoclonal mouse antiglutamate antibody (Incstar Corporation) diluted from 1/2,000 to 1/4,000 in PB with the addition of 1% normal pig serum. Following three washes in PB, the sections were incubated overnight in 2% biotinylated anti-mouse secondary antibody (Amersham), diluted in PBS containing 1% normal pig serum, and then incubated for 1 hour in streptavidine biotinylated peroxidase (Amersham). The final visualization of antigluamate immunoreactivity was made by reaction in DAB using one of the techniques given above, either with or without the addition of nickel-ammonium sulfate intensification. For light microscopy, sections were mounted on glass slides and counterstained with cresyl violet. For EM, nickel intensification was omitted, and sections were postfixed in 1% osmic acid, dehydrated in ethanol and acetone, embedded in Araldite, resectioned at 80 nm, contrasted with uranyl acetate and lead citrate, and studied in a Philips EM 301.

GAD immunohistochemistry. The protocol used to reveal anti-GAD immunoreactivity was similar to the procedure described above. Sections were incubated in primary anti-GAD antibody synthetized in goat (a gift of Dr. M. Tappaz), diluted from 1/2,000 to 1/10,000 in PBS containing 1% normal pig serum (for characterization and specifications of the antibody, see Oertel et al., 1981a,b; Berod et al., 1984; Denizot et al., 1987). After washing, the sections were incubated in a biotinylated secondary anti-goat antibody (Amersham), and labeling was revealed by using the DAB technique, as described above.

Combined glutamate and GAD immunohistochemistry. Anti-GAD immunoreactivity was revealed as above by using the DAB technique with nickel intensification. After incubation in the second antiglutamate antibody series, the DAB reaction was repeated without intensification. Thus, anti-GAD immunoreactivity appeared to be labelled blue/black, whereas elements showing antiglutamate immunoreactivity appeared to be brown.

GABA immunohistochemistry. For EM analysis of GABAergic elements in the ELL, a postembedding immunohistochemical technique was applied on thin sections obtained from material embedded at low temperature in Lowicryl HM20 resin. For this purpose, fish were anesthetized and perfused with 20 ml 0.9% NaCl followed by either 4% glutaraldehyde or a mixture of 2% paraformaldehyde and 2% glutaraldehyde in 0.1 M PB, pH 7.4. The brain was immersed overnight in perfusion fluid and sectioned at 100 or 200 μm on a Vibratome.

For freeze substitution and low-temperature embedding, the Vibratome sections were first treated with 0.1% sodium borohydride and 50 mM glycine (0.379 g/100 ml) in PB, pH 7.4. Next, they were cryoprotected by immersion in increasing concentrations of glycerol (10, 20, and 30%) in PB for 30 minutes for each concentration. The sections were oriented on pieces of Thermanox (LAB-TEK DVI; Miles Laboratories, Inc.) and were frozen rapidly by plunging in liquid propane (−190°C) using a rapid-freeze apparatus (KF80; Reichert-Jung, Germany). The propane was cooled with liquid nitrogen. After freezing, the specimens were transferred to the precooled chamber (−90°C) of a CS autofreeze-substitution apparatus (Reichert-Jung). Freeze substitution was performed as described by Müller et al. (1980). The tissue was immersed overnight in anhydrous methanol containing 0.5% uranyl acetate as fixing agent at −90°C. The temperature was raised stepwise 4°C per hour to −45°C. Prior to infiltration with Lowicryl HM20 resin (Bio-Rad, Richmond, CA), the tissue was washed several times with anhydrous methanol at −45°C to remove water and excess uranyl acetate. The embedding process was carried out at −45°C in three stages, with a progressively increasing ratio of resin to methanol. Diffuse UV-radiation (360 nm) was used to catalyze polymerization first at −45°C overnight and then at room temperature for 1 day. Thin sections were cut on a Reichert Ultracut-E and mounted on one-hole nickel grids coated with a Formvar film.

For postembedding GABA immunohistochemistry, ultrathin Lowicryl sections of the ELL were washed for 10 minutes in PBS, pH 7.4, containing 0.1% sodium borohydride and 50 mM glycine and for 10 minutes in PBS containing 0.5% BSA and 0.5% cold fish skin gelatine (PBG: PBS + BSA + CFSG = PBG, i.e., phosphate-buffered BSA-cold fish skin gelatine mixture). For immunolabeling, sections were incubated overnight at 4°C in drops of PBG containing a polyclonal anti-GABA antibody (obtained as a gift from Buijs; Amsterdam, Netherlands), diluted 1:6,000 (for characterization and specification of the antibody, see Seguela et al., 1984; Buijs et al., 1987, 1989). Sections were washed for 20 minutes in PBG and incubated in goat anti-rabbit immunoglobulin G (IgG)-labeled gold markers (10 nm; Aurion Wageningen, Netherlands). Sections were washed in PBS and postfixed with 2.5% glutaraldehyde in PBS for 5 minutes to minimize loss of gold label during the contrasting steps. After washing with distilled water, sections were contrasted in uranyl acetate and lead citrate and were studied by using a Philips EM 301 electron microscope.

Morphometric estimations

Several aspects of the neurons studied were quantified. Most parameters could be measured directly from the sections used, but determination of spine size and density using ultrathin sections required the application of some stereological formulae. For this purpose, we used an approach similar to that described previously for the mormyrid cerebellum (Meek and Nieuwenhuys, 1991). To calculate spine diameter, we used the formula

$$\overline{D} = \overline{d}\left[1 - \frac{(1 - 4/\pi)\,\overline{d}}{t + d}\right]$$

of Smolen et al. (1983), in which $\overline{D}$ is the average spine diameter, $\overline{d}$ is the average spine profile diameter in ultrathin sections, and t is the section thickness of 80 nm. To calculate densities and numbers, spine counts in ultrathin sections were corrected according to the modified Floderus

(1944)-Abercrombie (1946) formula

$$N_V = \frac{N_A}{\bar{D} + t - 2h}$$

in which N_A is the number of spines counted in a reference surface area, $\bar{D}$ is the spine diameter, t is the section thickness of 80 nm, and h is the height of lost caps of spines that are not recognizable in thin sections, as calculated by the formula

$$h = R - \sqrt{R^2 - r^2},$$

in which R is the mean particle radius, and r is the radius of the smallest profiles visible. The resulting value, N_V, represents the number of spines per reference volume. For estimations of the number of stellate (GABA-positive) synaptic contacts on the smooth surface of apical spiny dendrites, we used a formula that was adapted from Colonnier and Beaulieu (1985):

$$N_S = N_L/\bar{L},$$

in which N_L is the number of synaptic contacts counted along a certain dendritic membrane length, $\bar{L}$ is the average synaptic contact trace length, and N_s is the number of synaptic contacts per surface area of a dendrite.

RESULTS

ELL zones and layers

The present study will employ the terminology developed by previous investigators (Maler, 1973; Bell et al., 1981), with some adaptations. Accordingly, the ELL cortex is subdivided into the MZ, the DLZ, and the VLZ, zones that are separated clearly by septa consisting of glial tissue. The MZ and the DLZ together are called the *mormyromast zones*, because they process primary afferent input from mormyromasts, whereas the VLZ processes ampullary input (Bell and Szabo, 1986). The present study is restricted to the mormyromast region of the ELL.

In line with previous studies, we distinguish six main ELL layers, from superficial to deep: the molecular (mol), ganglionic (gangl), plexiform (plex), granular (gran), intermediate (int), and deep fiber (deep) layers (Fig. 1). However, the boundary between the granular layer and the intermediate (cell and fiber) layer differs from that designated by previous authors, because our granular layer includes the superficial part of the intermediate cell and fiber layer of Maler (1973). The superficial and deep parts of our granule layer, as will be discussed below, have a number of striking features in common, whereas they differ clearly from the deeper located intermediate cell and fiber layer.

Morphology of ELL projection neurons

It has been shown previously that the ELL projects via the lateral lemniscus to the lateral nucleus of the torus semicircularis, with an additional, probably collateral projection to the preeminential nucleus (Bell et al., 1981). Cells in ELL that are labeled retrogradely by HRP application to the lateral toral nucleus, thus, have been called *lemniscal projection neurons* in the present study. This term allows for a distinction from other types of projection neurons, particularly those projecting to other ELL zones, either ipsilaterally (interzonal) or contralaterally (intrazonal or commissural). The results of HRP application to the lateral toral nucleus show that retrogradely labeled lemniscal projection neurons occur in several layers of the ELL, with the highest density in the ganglionic and granular layers (Figs. 2, 3).

In the ganglionic layer, the projection neurons are the largest elements, and will be indicated as *large ganglionic* (LG) cells. They appear to be located preferentially in the deeper part of the ganglionic layer, close to the boundary with the plexiform layer, and they have a spherical cell body. Their soma diameter, as measured after HRP labeling, is about 14 μm in the MZ (14.4 ± 2.4 μm width × 13.1 ± 2.2 μm height; n = 33) and about 13 μm in the DLZ (12.2 ± 1.9 × 13.8 ± 2.2; n = 67). LG cells give rise to several (generally two or three) apical dendrites that branch in the transition zone between the ganglionic and molecular layer and that continue far into the latter (Fig. 4a–c). In addition, these cells have a number of relatively thin, short basal dendrites located in the plexiform layer and its boundaries (Figs. 3, 4).

Retrogradely labeled lemniscal projection neurons situated in the granular layer deviate significantly in shape from LG cells, because their cell body is fusiform rather than spherical. The frequency of occurrence of these neurons, called *large fusiform* (LF) cells, is largest in the superficial granular layer, where they measure 10.5 ± 1.5 × 19.7 ± 4.3 (n = 32) in the MZ and 10.4 ± 1.6 × 21.1 ± 4.7 (n = 45) in the DLZ after HRP labeling. In the deep granular layer LF neurons are slightly smaller and more spherical (MZ: 11.5 ± 1.8 × 17.4 ± 2.6; n = 16; DLZ: 10.0 ± 3.8 × 18.3 ± 4.5; n = 7). They tend to be located preferentially in boundary regions of the granular layer (i.e. between the plexiform and granular layers, between the superficial and deep granular layers, and between the granular and intermediate layers; Fig. 2), but intermediate positions occur as well. LF cells have one or two stout apical dendrites that generally originate from the soma without a distinct transition (Figs. 3, 4). These apical dendrites branch first in the transition zone between the plexiform and ganglionic layers and then again at the level of transition between the ganglionic and molecular layers. Additional branches may arise more superficially in the molecular layer (Fig. 4). The basal pole of LF cells gives rise to a number of small basal dendrites, which led to them being called "beard" cells by Maler (1973). However, because LG cells, which were not described by Maler (1973), also have a beard, we prefer the name *large fusiform cells*. Apart from their location, it is the shape of the soma and not the presence of basal dendrites that distinguishes LF cells from LG cells.

HRP application to the lateral line nerve shows that, in both the MZ and the DLZ, primary afferent input terminates exclusively in the granular layer (Fig. 5) both in its superficial and deep parts, thus confirming previous results (Bell et al., 1989). This strongly suggests that the different shapes and locations of LG and LF cells are correlated with different synaptic inputs and different functions in ELL circuitry: LF cells might well have direct contact with primary afferents, whereas LG cells do not, because their basal dendrites in the plexiform layer are not in a position to make synapses with primary afferent terminals (cf. Figs. 3–5).

In addition to the LG and LF cells just described, a few retrogradely labeled lemniscal projection neurons are also found in the plexiform and intermediate layers (Figs. 2, 3). Those in the plexiform layer are either spheroidal or fusiform and sometimes have intermediate properties. A more detailed knowledge of their synaptic input would be necessary to decide whether these cells represent displaced LF and/or LG cells or whether they should be considered as a distinct population of lemniscal projection neurons. The

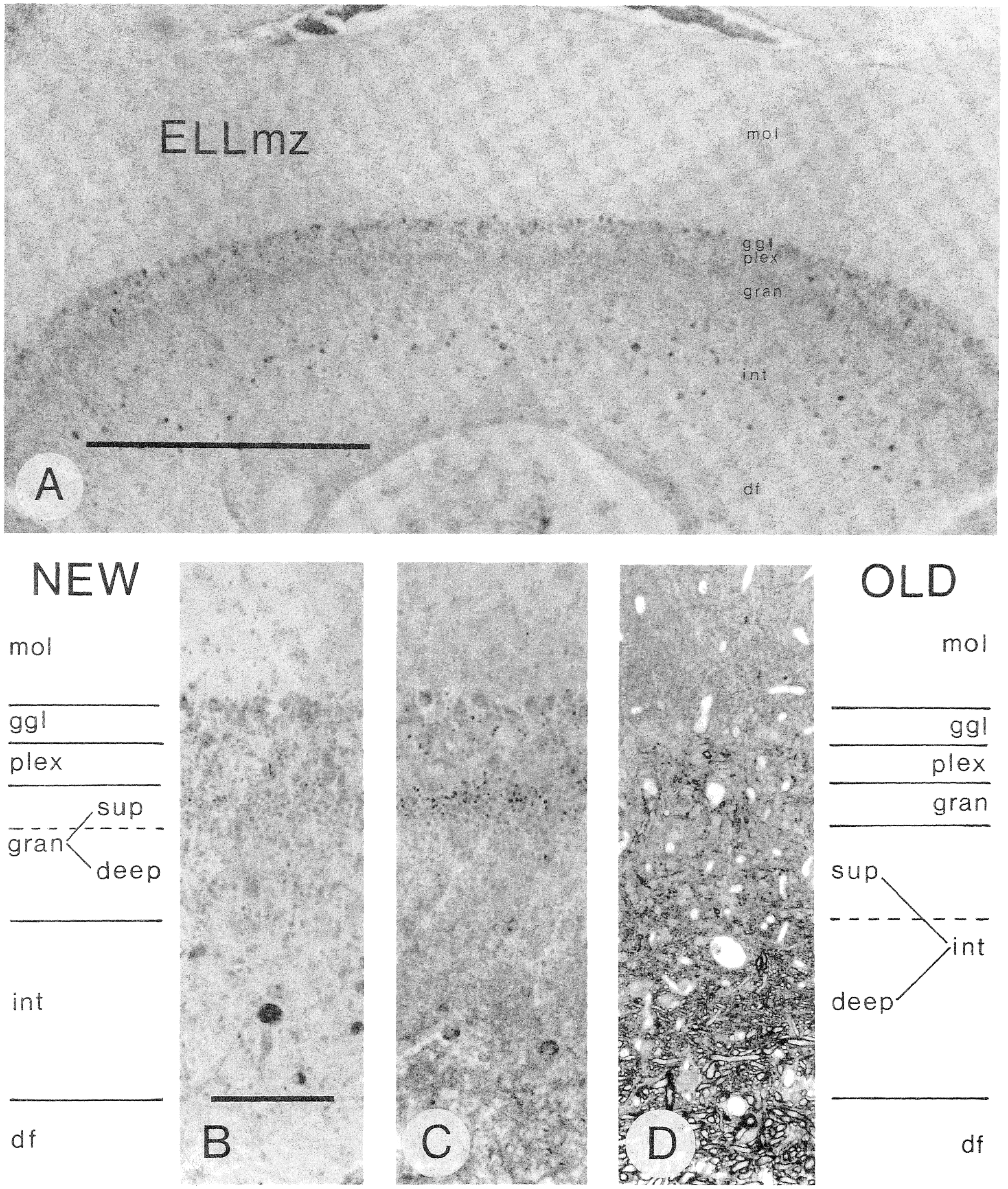

Fig. 1. The layers of the mormyrid electrosensory lateral line lobe (ELL) as visible in Nissl- (**A,B**) and Kluver-Barrera-stained (**C**) 15 μm paraffin sections and in a Methylene-blue stained 2 μm plastic-embedded section (**D**). Note that the granular and intermediate layer distinguished in the present study (indicated on the left) differ from those distinguished previously (indicated on the right). df, Deep fiber layer; ggl, ganglionic layer; gran, granular layer; int, intermediate (cell and fiber) layer; mol, molecular layer; plex, plexiform layer. Scale bars = 500 μm in A, 100 μm in B–D.

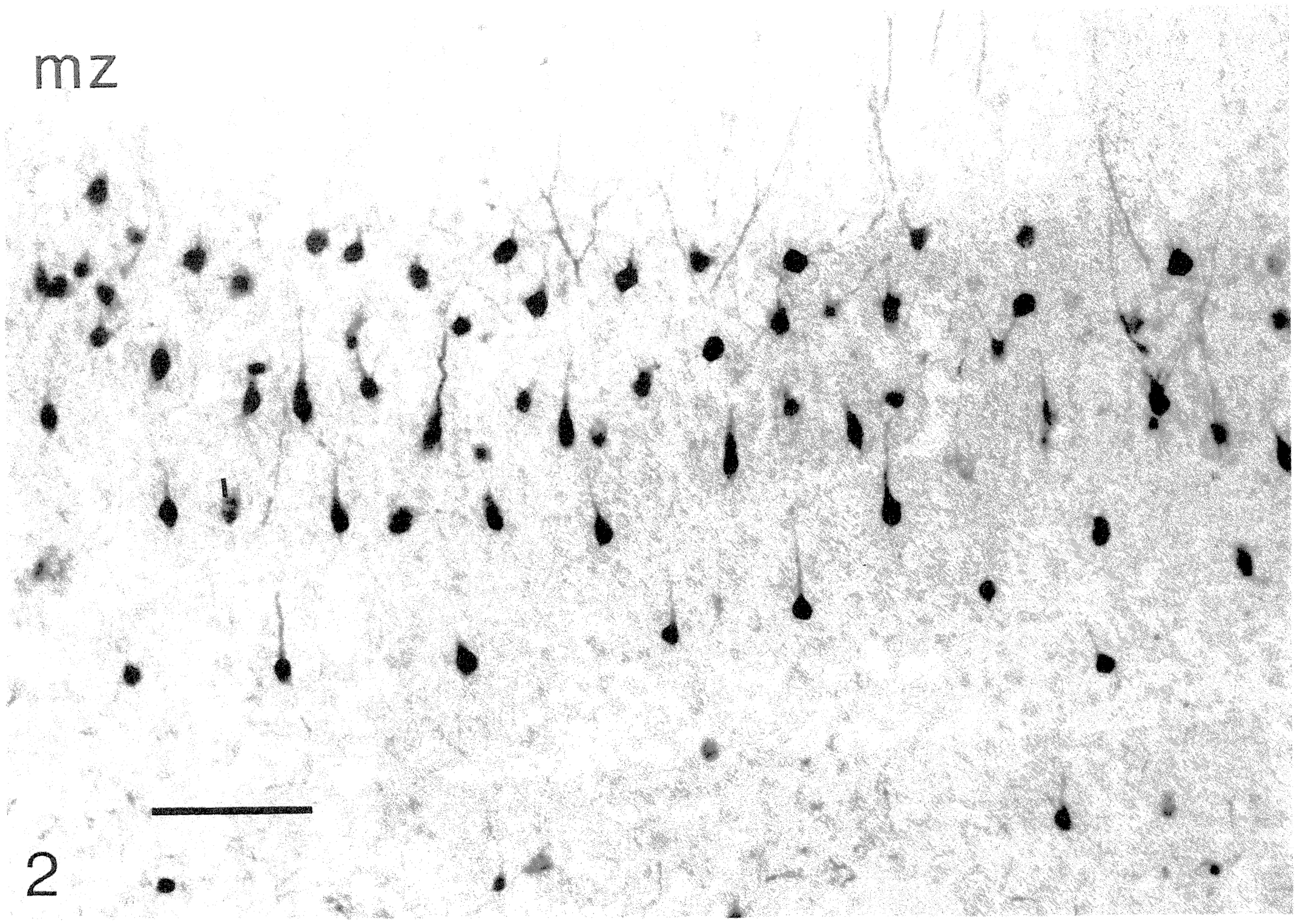

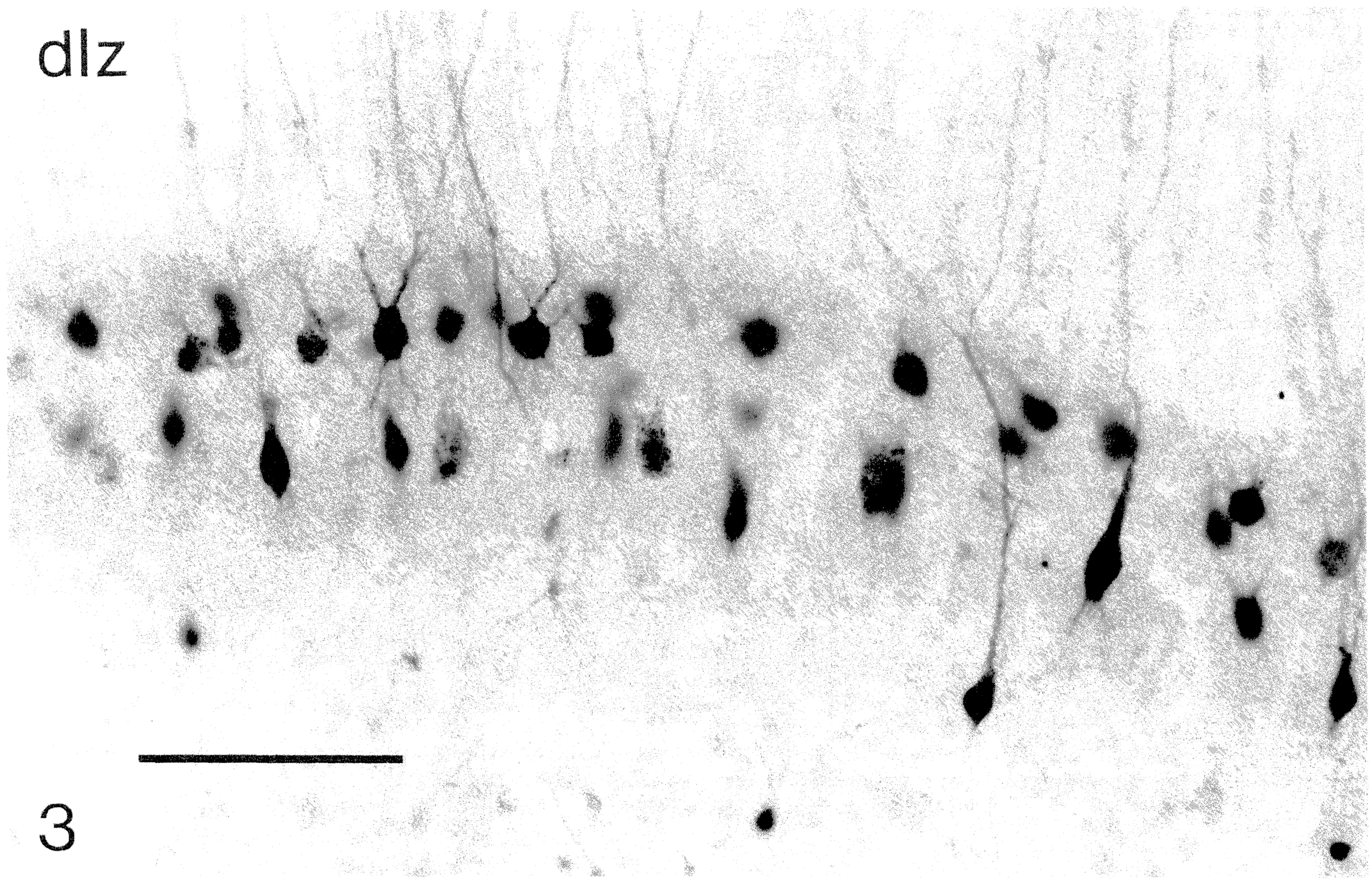

Figs. 2, 3. Retrogradely labeled lemniscal projection neurons in the medial zone (Fig. 2) and dorsolateral zone (Fig. 3) of the mormyrid ELL following horseradish peroxidase (HRP) injection in the lateral nucleus of the torus semicircularis. mz, Medial zone. dlz, dorsolateral zone. Scale bars = 100 μm.

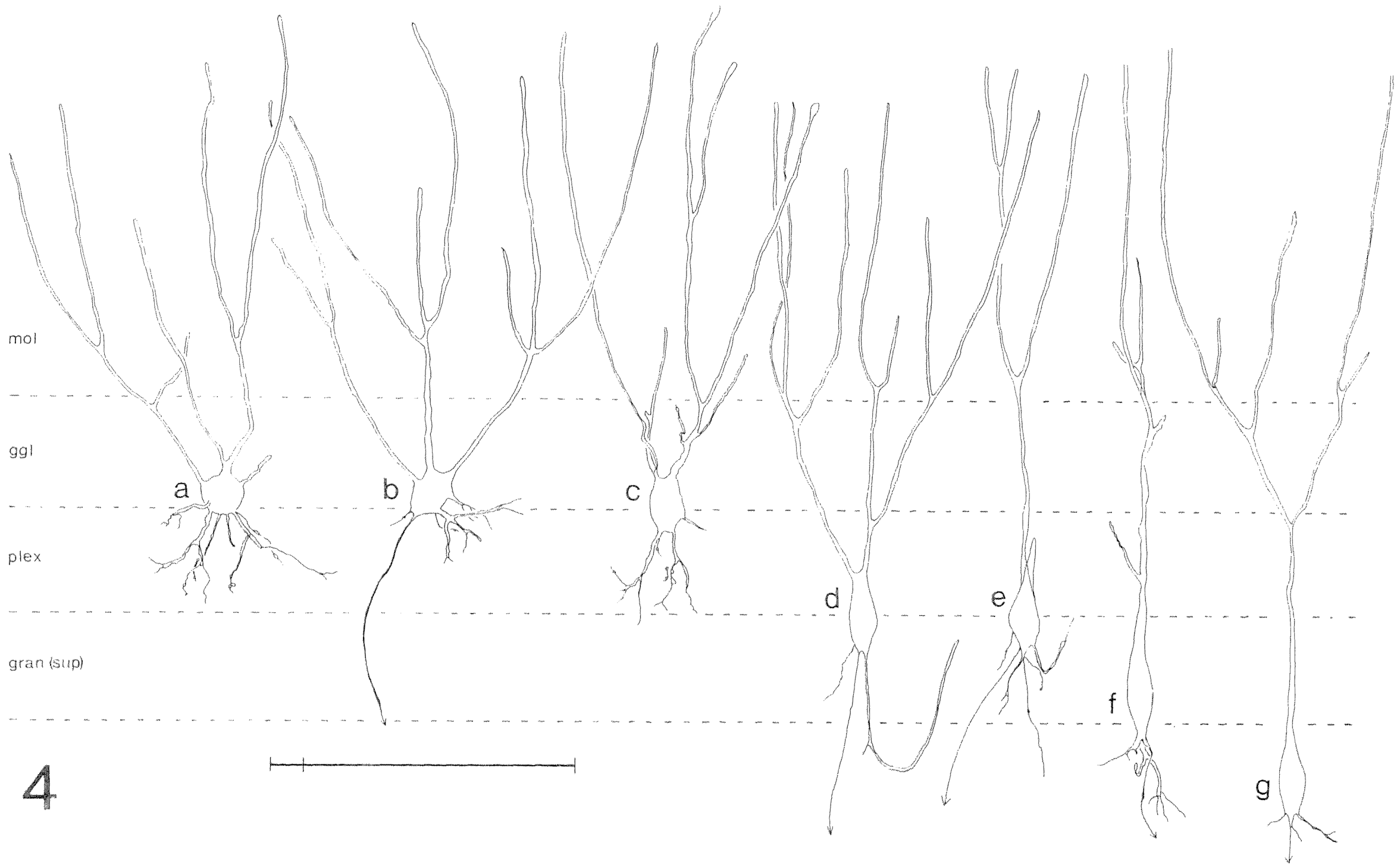

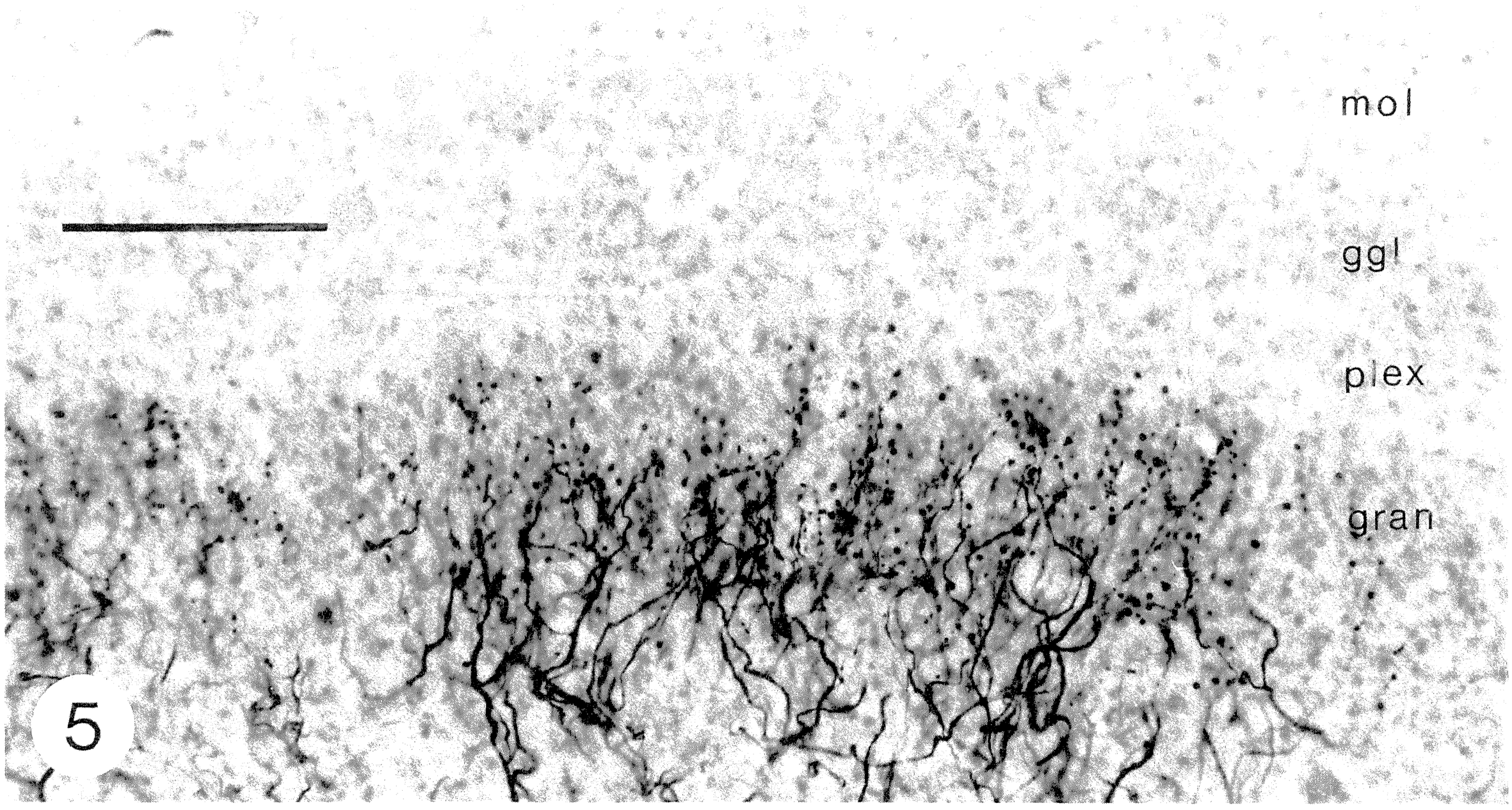

Fig. 4. Composite drawing of some of the most completely HRP-labeled projection neurons of the dorsolateral zone of the mormyrid ELL, including large ganglionic neurons (**a–c**) and superficially (**d,e**) as well as more deeply (**f,g**) located large fusiform neurons. Scale bar = 100 μm.

Fig. 5. HRP-labeled mormyromast primary afferents in the dorsolateral zone of the mormyrid ELL showing the exclusive location of terminals in the granular layer. Scale bar = 100 μm.

few lemniscal projection neurons observed in the intermediate cell and fiber layer are relatively small. Because details of their precise morphological properties are presently lacking, they will not be considered further here.

Details of the dendritic organization of LG and LF cells were studied by using intracellular labeling and Golgi impregnation. In the MZ, these neurons have 6–12 apical dendrites that establish a dendritic tree about 250 μm in diameter in the transverse plane (Figs. 6–8). Their rostrocaudal field diameter may be somewhat greater, because they sometimes extend throughout the complete thickness of the 400 μm slices used for in vitro intracellular fills. However, they are certainly not as flattened as cerebellar Purkinje cells. In the DLZ, the dendritic fields of LF and LG cells are narrower, although they are established by a similar number of dendrites (Fig. 6g–i).

The diameters and branching patterns of the apical dendrites of LG cells are rather variable: Some dendrites are rather thin over their whole length, others are quite thick, and still others are thin at their origin but become quite thick at some distance from the soma (Fig. 6). Most primary dendrites branch once or twice after their origin from the soma, giving rise to two to four distal dendrites, although others remain unbranched (Fig. 6). The apical dendrites of LF cells branch once or twice more, because most of them originate from a single apical dendrite, as described above. Their diameters seem to be less variable than those of LG cells.

Remarkably, not all LG and LF cells have dendrites that continue up to the superficial molecular layer (Figs. 6–8). In Golgi-impregnated material, this might be due to incomplete impregnation or sectioning at the surface of the 100-μm-thick section. However, from wholemounts of intracellularly filled cells, it can be seen that some LF and LG cells have apical dendrites that are well filled and are not located at the surface of the slices but that still are clearly restricted to the deeper part of the molecular layer (Fig. 6c,d,f). Dendrites of these cells frequently terminate with a growth cone-like swelling (Fig. 6d′, asterisk), but it is uncertain whether these are really dendritic growth cones or another type of terminal specialization or artefact (see Discussion). Similar configurations are also visible sometimes in Golgi-impregnated cells (Fig. 7, asterisks).

Although dendritic spines are only sometimes visible following retrograde labeling with HRP or in intracellular fills of LF and LG cells, Golgi impregnations demonstrate the presence of these specializations on the apical dendrites of both LF and LG cells quite clearly (Figs. 7, 8). Spines are generally absent on the proximal part of the dendrite but begin to appear in the ganglionic layer (LF cells; Fig. 7) or in the deep molecular layer (LG cells; Fig. 8). In the molecular layer, 60–180 spines per 100 μm length can be counted on thin and thick dendrites, respectively, although it should be mentioned that spine density is not related strictly to dendrite diameter. However, previous Golgi studies have shown that spine counts on Golgi-impregnated cells yield serious underestimations and that real spine numbers for thick dendrites may be up to three times higher, because most spines in Golgi preparations are masked by their parent dendrite (Meek and Nieuwenhuys, 1991). This means that spine density on LG and LF apical dendrites may range from 100 to 500 per 100 μm length for thin and thick dendrites. Consequently, dendrites extending about 400 μm from the deep to the superficial molecular layer may have 400–2,000 spines, and neurons with six to ten dendrites (Fig. 6) may bear a total of about 2,500–20,000 spines.

The basal dendrites of both LF and LG cells are nonspiny and rather short. Both intracellular labeling and Golgi impregnation show that their organization is quite variable. In some cells, a large number of small thin dendrites arise directly from the soma, whereas other neurons also have a few thicker basal dendrites that give rise to additional side branches. The longest (and thickest) basal dendrites extend about 100 μm. Together, the basal dendrites of all lengths and diameters establish a dendritic field no more than 150 μm in diameter (Figs. 7, 8). Tangential sections through the caudal part of the ELL MZ reveal that these dendritic fields extend concentrically all around the soma (Fig. 9). Similar to the results of retrograde HRP transport, Golgi impregnations and intracellular labeling show that the basal dendrites of LG cells are restricted to the ganglionic and plexiform layers, whereas LF cells extend their dendrites into the granular layer and its boundaries (Figs. 6–8). A few cells have an intermediate position (see, e.g., Fig. 8d).

The axonal properties and projections of lemniscal projection neurons, including LF and LG cells, and also a minor population of small intermediate layer cells were studied by using injections of the anterograde tracer PHA-L into the ELL. These resulted in labeled axons that projected via the lateral lemniscus to the preeminential nucleus and the lateral nucleus of the torus semicircularis, thus confirming previous retrograde tracer experiments (Bell et al., 1981; Finger et al., 1981). A few additional terminals were observed in the region ventral to the decussation of the lateral lemniscus and in the ventral posterior toral nucleus (Fig. 10). The projections to the preeminential nucleus were clearly collaterals from the ELL-toral axons, because the number and diameter distribution of the labelled axons in the lateral lemniscus rostral and caudal to the preeminential nucleus was always the same in any given experiment.

Within the lateral toral nucleus, terminals are located in restricted regions, agreeing with the topographic organization described previously (Bell et al., 1981; Finger et al., 1981). The terminals are concentrated frequently in small clusters (Fig. 12). EM analysis of such clusters shows that they contain terminals with large round vesicles and asymmetrical synaptic contacts, suggesting an excitatory influence on their small dendritic targets (Figs. 11–13). This fits with the immunohistochemical characterization of LG and LF cells.

Immunohistochemistry

Treatment with antibodies against glutamate reveals a population of strongly immunopositive large cells in the ganglionic and granular layers (Fig. 14). Comparison of their size, shape, and dendritic branching pattern with the description presented above leaves no doubt that these glutamatergic elements are the multipolar LG cells and the fusiform LF cells. A few smaller elements, particularly in the deep molecular layer and the granular layer, appear to be glutamate-positive as well (Fig. 14). Those in the deep molecular layer probably represent the deep molecular layer cells that are described in the accompanying paper (Meek et al., 1996). Because the glutamate antibody penetrates only a few microns, glutamate immunohistochemistry gives a good impression of the frequency of occurrence of LF and LG cells in a thin sheet of ELL tissue (Fig. 14). It appears that LG and LF cells have a similar frequency of

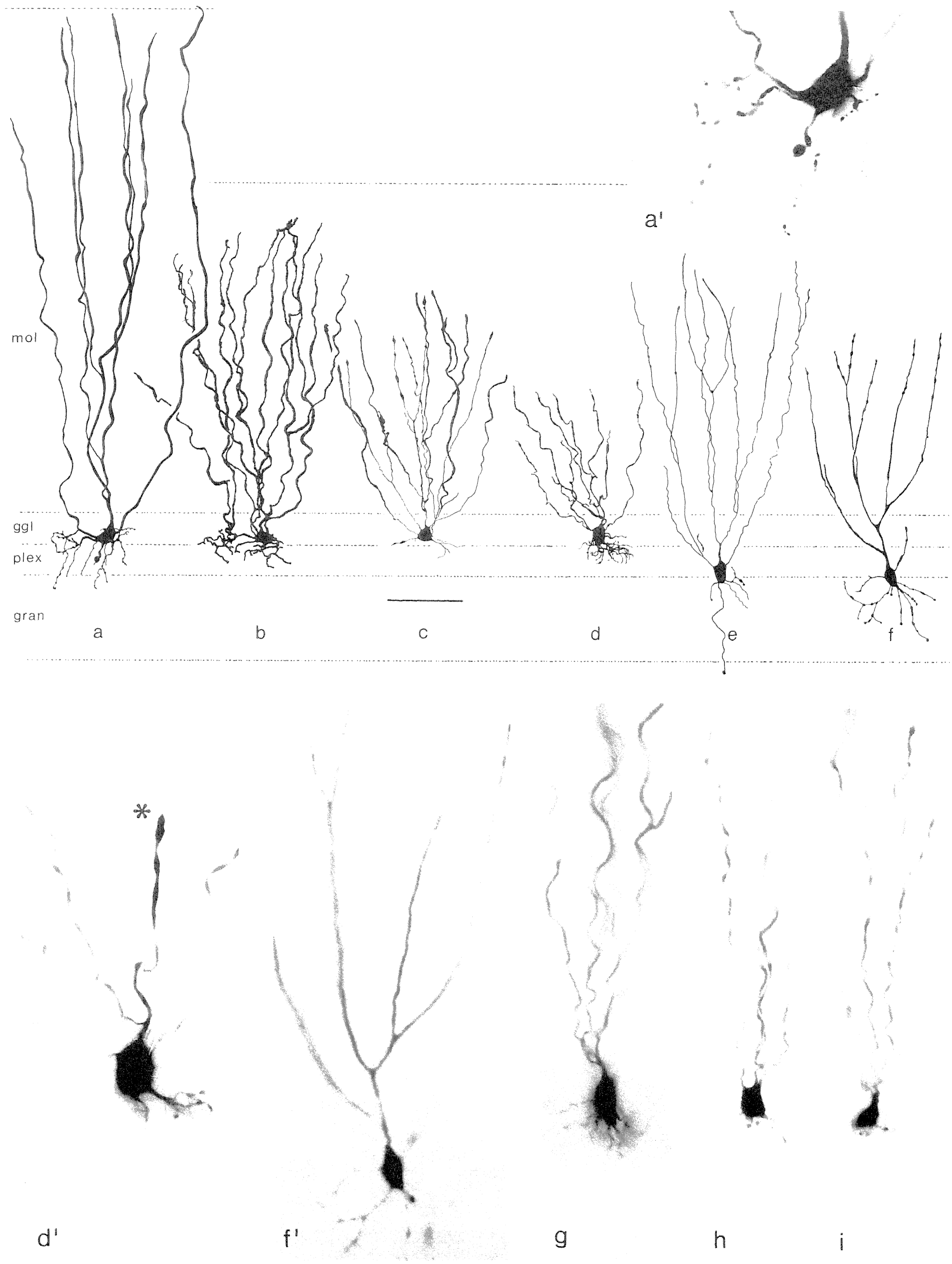

Fig. 6. Drawings and photographs showing intracellularly labeled large ganglionic (**a–d**, **g–i**) and large fusiform (**e,f**) neurons in the medial zone (a–f) and the dorsolateral zone (g–i) of the mormyrid ELL. **a′,d′,f′**: Details of a, d, and f, respectively. The asterisk in d′ indicates a growth cone-like dendritic tip. Scale bar = 100 μm.

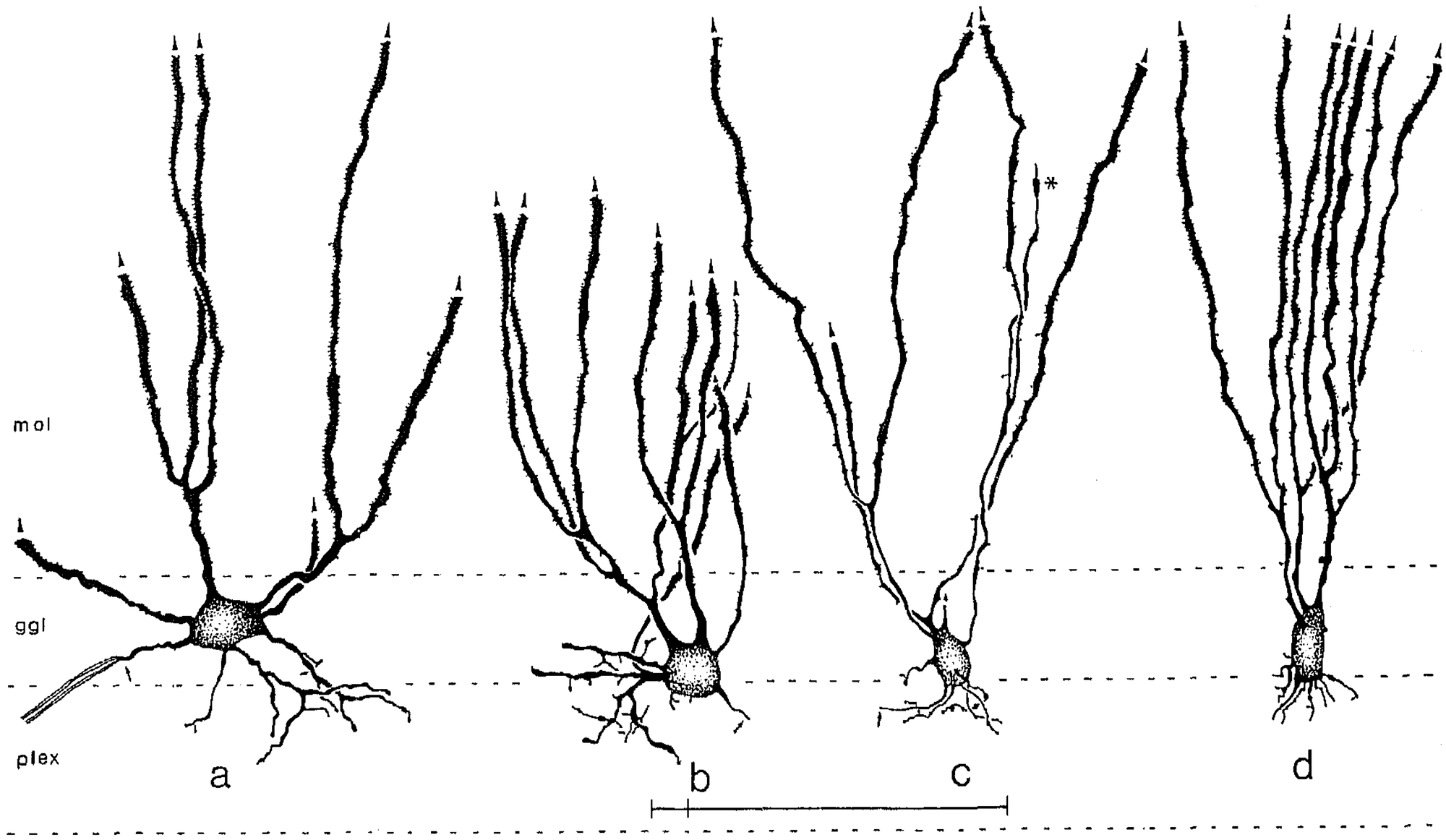

Fig. 7. Composite drawing of Golgi-impregnated large ganglionic layer cells in the medial (**a–c**) and dorsolateral (**d**) zones of the mormyrid ELL. Arrowheads indicate structures that continue but that were not drawn further, because they ran out of the section(s) studied or out of the frame of the drawing. Arrows point to axons, and the asterisk indicates a growth cone-like dendritic tip. Scale bar = 100 μm.

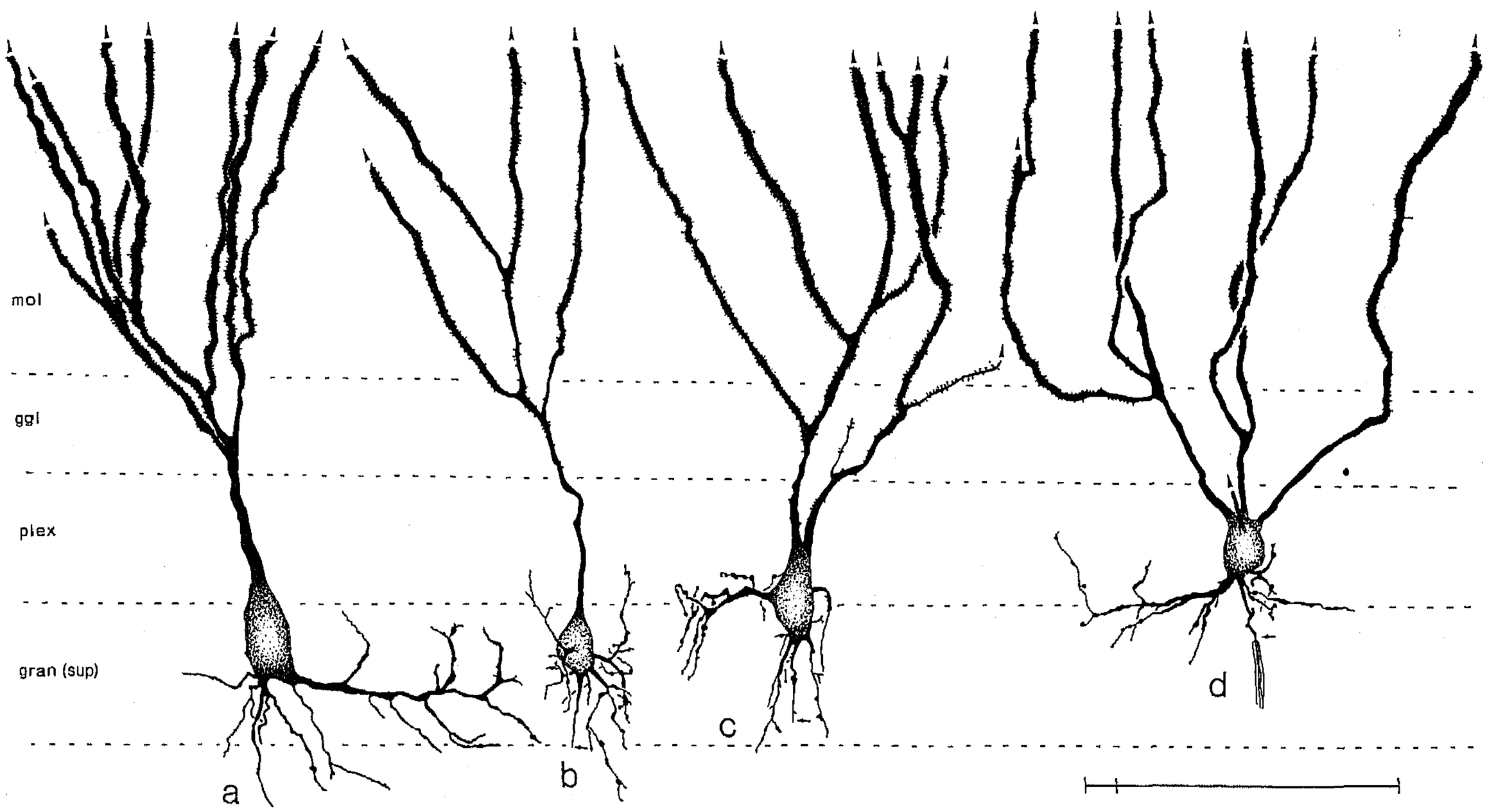

Fig. 8. Composite drawing of Golgi-impregnated large fusiform cells (**a–c**) and a cell (**d**) with properties that are intermediate between large fusiform and large ganglionic layer cells (see text). Arrows and arrowheads are as explained for Figure 7. Scale bar = 100 μm.

occurrence in the MZ, whereas their ratio in the DLZ is about 2:1. More precise morphometric procedures are necessary to determine their exact ratios and to test the apparent difference between the MZ and DLZ statistically, but global impressions from HRP material (Figs. 2, 3) and GABA immunohistochemistry (see Meek et al., 1996) are similar. The latter also shows that LG cells represent no more than about 2% of the cells in the ganglionic layer, both

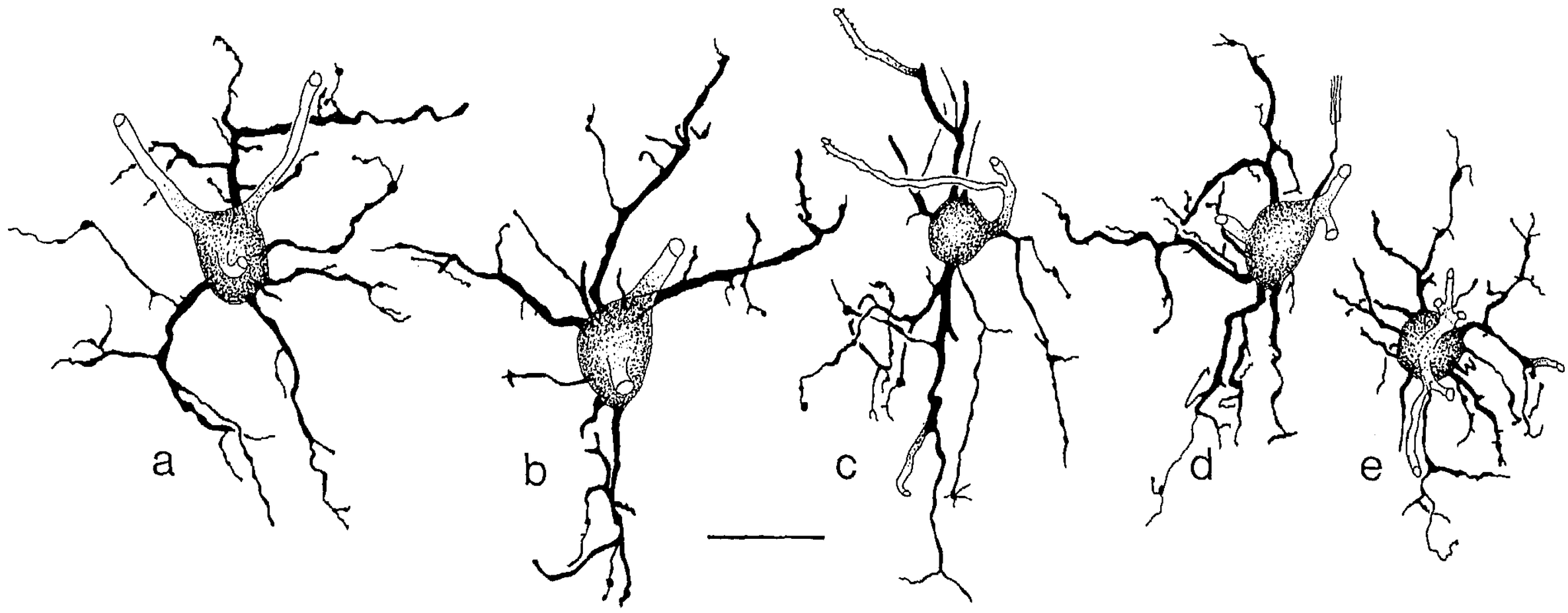

Fig. 9. **a–e:** Tangential view of five Golgi-impregnated large ganglionic layer cells showing the extension and orientation of their basal dendrites in the plexiform layer (drawn in black). The proximal apical dendrites have been drawn in white. Scale bar = 25 μm.

in the MZ and DLZ. Most cells in the ganglionic layer appear to be smaller and GABAergic (Meek et al., 1996).

Combination of glutamate and GAD immunohistochemistry reveals that both LG and LF cells are densely covered with GAD-positive terminals (Figs. 15, 16), whereas other neurons in the ganglionic, plexiform, and granule layers are not. This, in addition to their size, is a useful criterion for distinguishing LF and LG cells in normal EM preparations. The high density of GAD-positive terminals occurs on the soma as well as on the proximal apical and basal dendrites of LG and LF cells (Figs. 15, 16).

Electron microscopy

The synaptic organization of LG and LF cells was investigated by using combined immunohistochemical (glutamate and GABA) and EM techniques. EM analysis of material treated with preembedding glutamate techniques confirms the conclusions drawn from LM analysis that LG and LF cells are the largest elements in the ganglionic and granular layers and are densely covered with synaptic boutons (Fig. 17, 18). Postembedding GABA immunohistochemistry confirms that most terminals are GABAergic (Fig. 19), making symmetrical synaptic contacts and containing small pleiomorphic vesicles (Fig. 20). They occur on the soma as well as on the basal dendrites of LF and LG cells (Figs. 17–21, 24, 25). Only a few non-GABAergic terminals with spherical vesicles, probably representing excitatory elements, occur on the smooth surface of their soma and proximal dendrites, contributing, maximally, to 5% of the somatic synaptic contacts of LG and LF cells. In a series of fortunate EM sections, the axon of one LF cell could be followed until its myelinated continuation, thus confirming that the parent cell was indeed a projection neuron.

The spiny apical dendrites of LF and LG cells in the molecular layer are intermingled with spiny dendrites of other elements and, thus, cannot be identified in normal EM material. However, in combination with immunohistochemistry, they can be indentified either positively (using glutamate antibodies) or negatively (using GABA antibodies), because all other spiny dendrites in the molecular layer appear to be GABAergic. The spines of GABA-negative spiny dendrites in the molecular layer make large numbers of synaptic contacts with GABA-negative terminals and have, in addition, a substantial number of GABA-positive synaptic contacts on their smooth surface (Fig. 22, 23). The latter probably arise from GABAergic stellate cells that could be identified in the same sections throughout the molecular layer.

Spines of GABA-negative dendrites in the molecular layer of the ELL have an average profile diameter of 0.24 μm in our material, which means an average spine diameter of 0.29 μm with a maximum of 0.39 μm. We counted 17.6 ± 6.0 spines per 100 μm along the surface of GABA-negative dendrites, from which an average density of 64 spines per 100 μm^2 surface can be calculated after correction for spine diameter, section thickness, and spine distance. Because the diameter of GABA-negative dendrites in the EM is 1.27 ± 0.34 μm, which implies an average circumference of 4.00 μm, this means that there are 256 ± 83 spines per 100 μm dendritic length. This is in agreement with predictions based on Golgi-impregnated material (see above). The density of GABA-positive (presumably stellate) synaptic contacts on the smooth surface of GABA-negative spiny dendrites in the molecular layer is about 19 per 100 μm^2 surface, which means approximately 75 per 100 μm dendritic length, 300 per dendrite 400 μm long, and 2,500–3,500 per LF or LG neuron. The ratio between spiny (excitatory) and nonspiny (inhibitory) contacts is approximately 10:3 for non-GABAergic spiny dendrites in the molecular layer. Because apical dendrites of LG and LF cells cannot be distinguished from one another in the EM without serial section and reconstruction, we do not know whether there are significant differences between the two types in this respect.

DISCUSSION

The morphological, synaptic, and immunohistochemical properties of the projection neurons of the mormyrid ELL are summarized in Figure 26 and were studied here by using a variety of complementary techniques at the LM and EM levels. This semiquantitative schematic representation is based on figures for the relative numbers of different cell

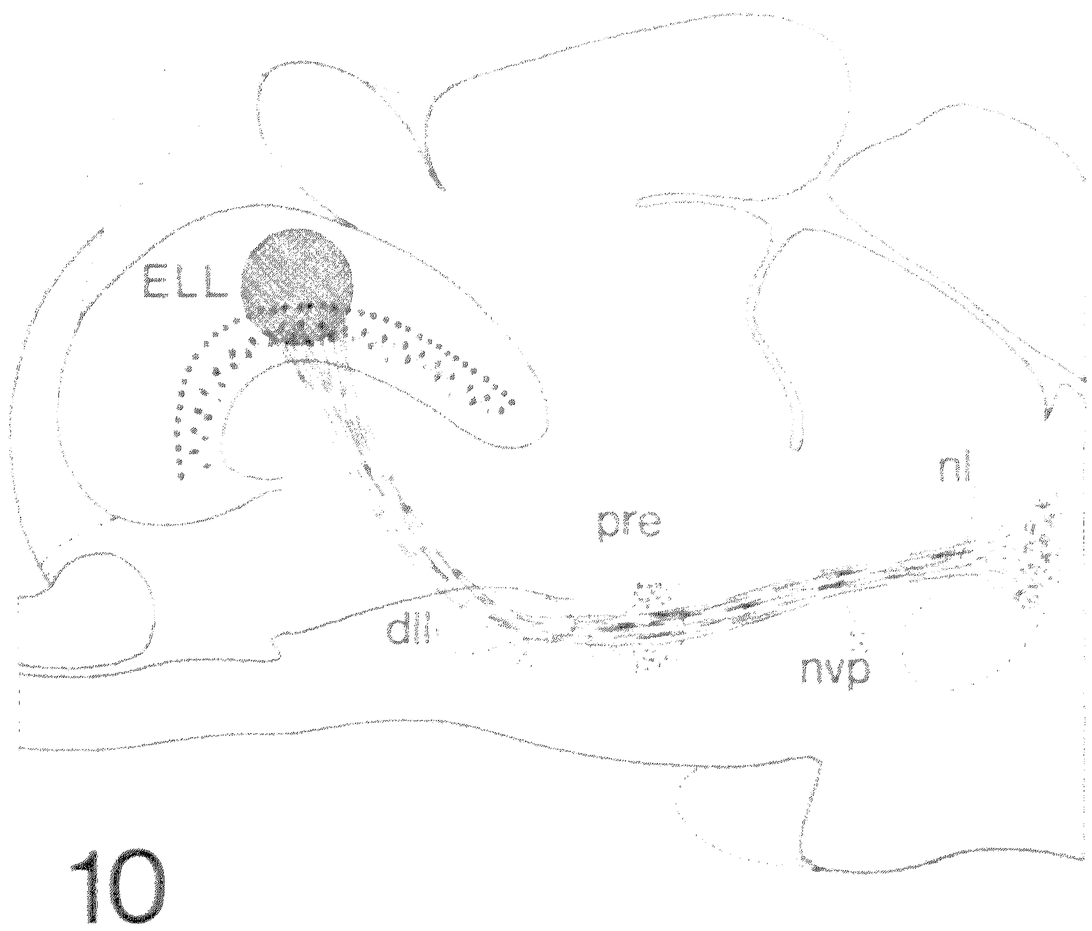

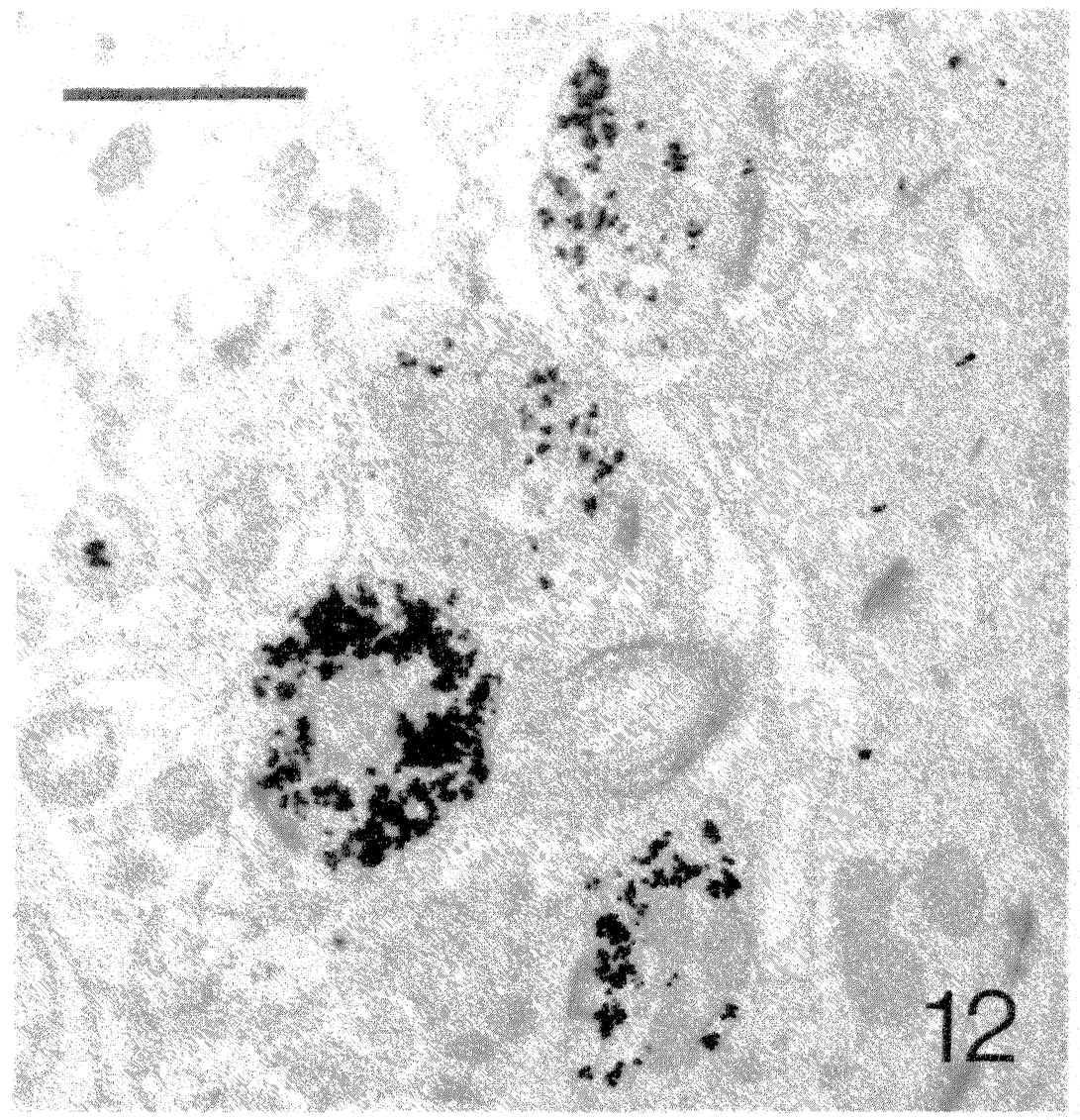

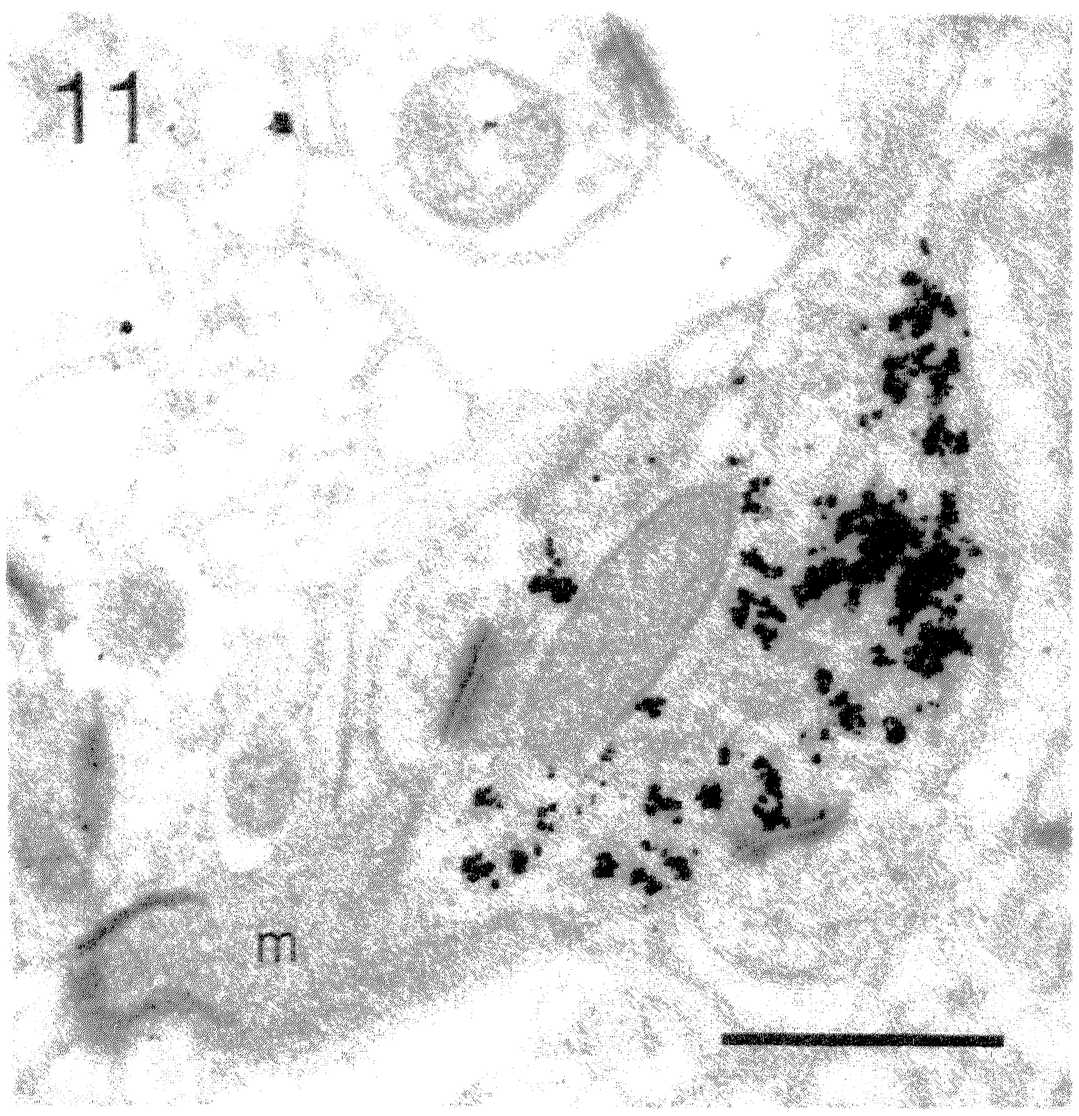

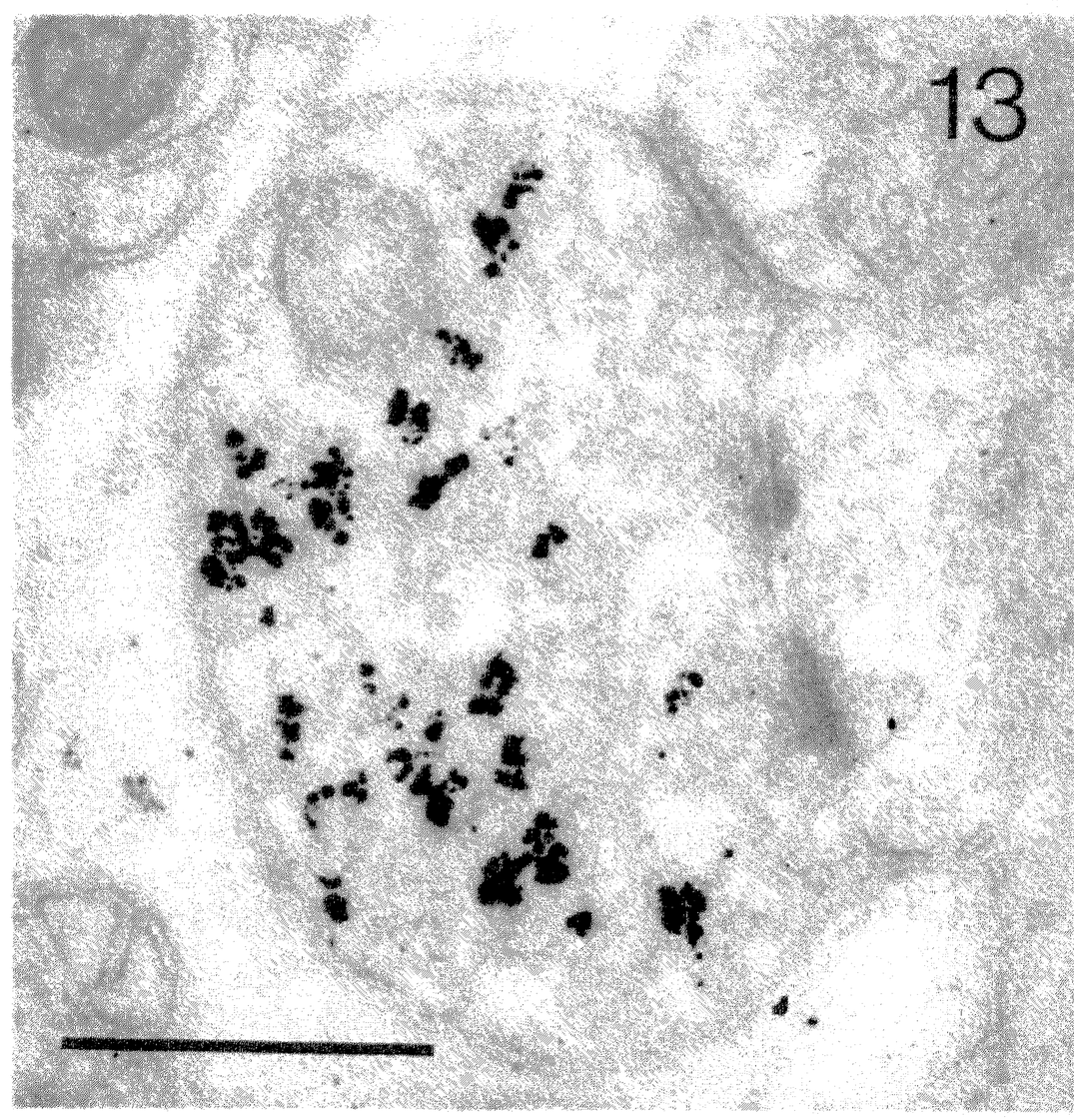

Figs. 10–13. Results of anterograde labeling of lemniscal ELL efferents after *Phaseolus vulgaris*-leucoagglotinin (PHA-L) injection in the medial ELL zone.

Fig. 10. A schematic drawing of the lemniscal course of ELL efferents and of the location of terminals under the decussation of the lateral lemniscus (dll) and in the preeminential nucleus (pre), the nucleus ventralis posterior of the torus semicircularis (nvp), and the lateral nucleus of the torus semicircularis (nl).

Fig. 11. A PHA-L labeled terminal in the lateral toral nucleus arising from a myelinated axon (m, myelin) and making two asymmetrical synaptic contacts with small dendritic profiles. Scale bar = 0.5 μm.

Fig. 12. A cluster of PHA-L labeled terminals in the lateral toral nucleus intermingled with several unlabeled terminals. Scale bar = 1 μm.

Fig. 13. Detail of a section neighboring Figure 12 showing the upper labeled terminal with its large round vesicles, asymmetric synaptic contacts, and glial encapsulation at high magnification. Scale bar = 0.5 μm.

types, their morphological features, and synaptic contacts in the MZ of the ELL. The basic organization of the projection neuron population is also very similar in the DLZ of ELL, but the present analysis shows that there are relatively more LF than LG neurons in the DLZ (LG:LF = about 1:1 in the MZ but about 1:2 in the DLZ) and that all

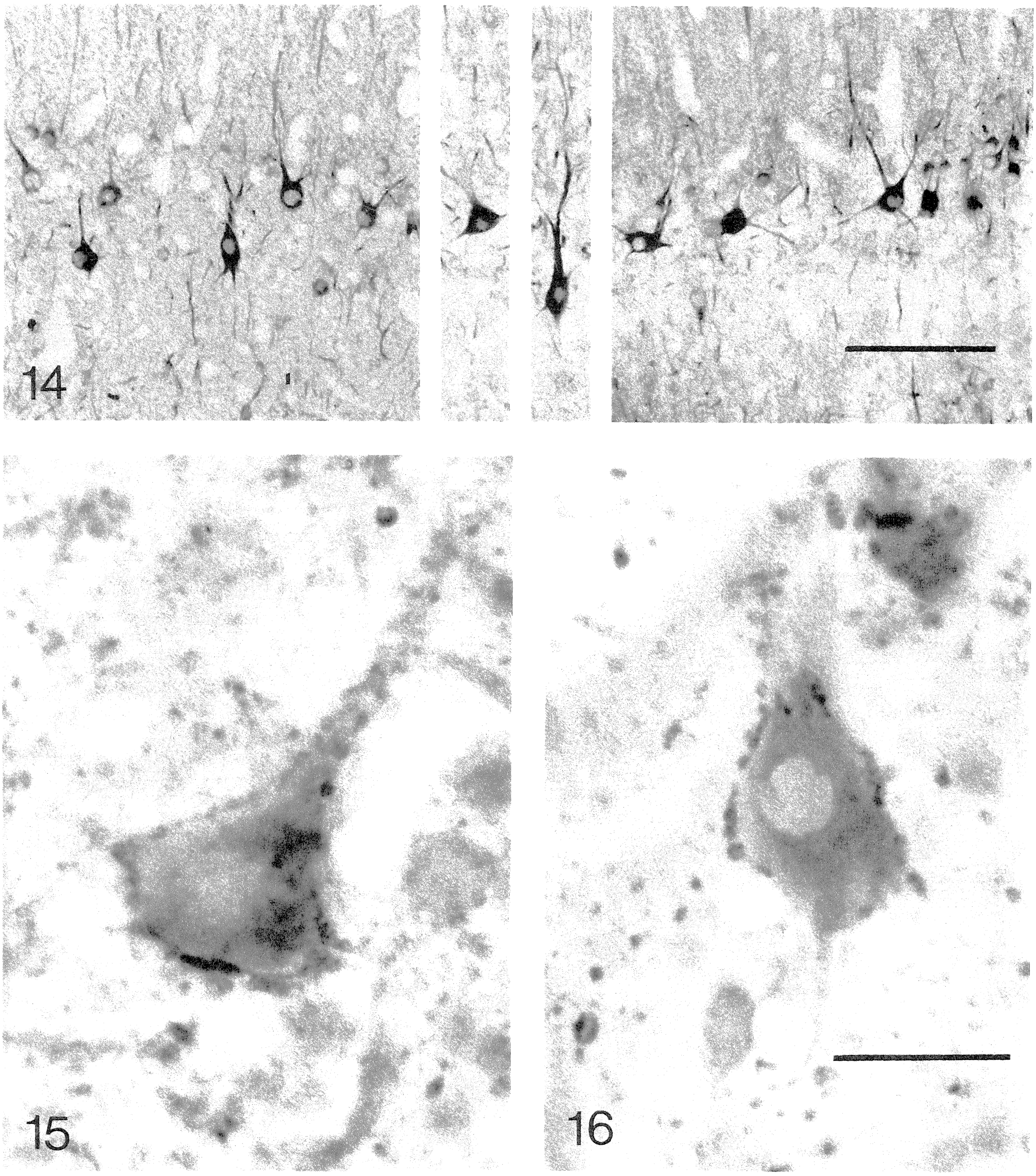

Figs. 14–16. Light microscope pictures of glutamate-immunoreactive elements in the mormyrid ELL. Figures 15 and 16 are photographs of a section that was treated for combined glutamate immunohistochemistry [visualized with a brown 3,3′-diaminobenzidine (DAB) precipitate] and γ-aminobutyric acid decarboxylase (GAD) immunohistochemistry (visualized by a blue-black DAB-Ni precipitate) showing that both glutamate-positive large ganglionic cells (Fig. 15) and large fusiform cells (Fig. 16) are surrounded by GAD-positive terminals. Scale bars = 100 μm in Figure 14, 20 μm in Figures 15, 16.

projection neurons in the DLZ have somewhat smaller somata and a more condensed apical dendritic arborization. For a more complete functional analysis of the differences between the MZ and DLZ, in which primary afferent fibers of different origins terminate (Bell et al. 1989; Bell 1990b), a more detailed morphometric study will be necessary.

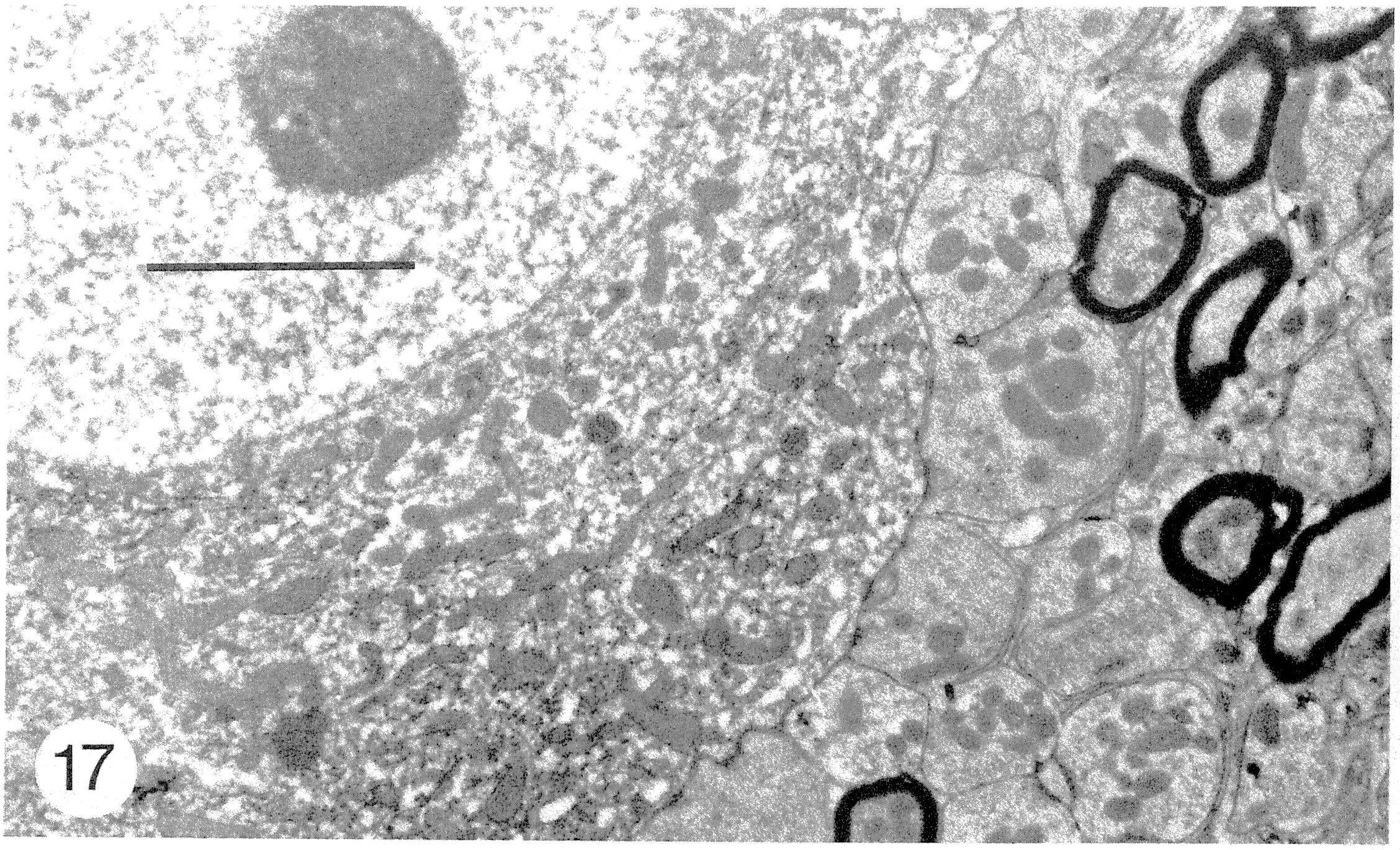

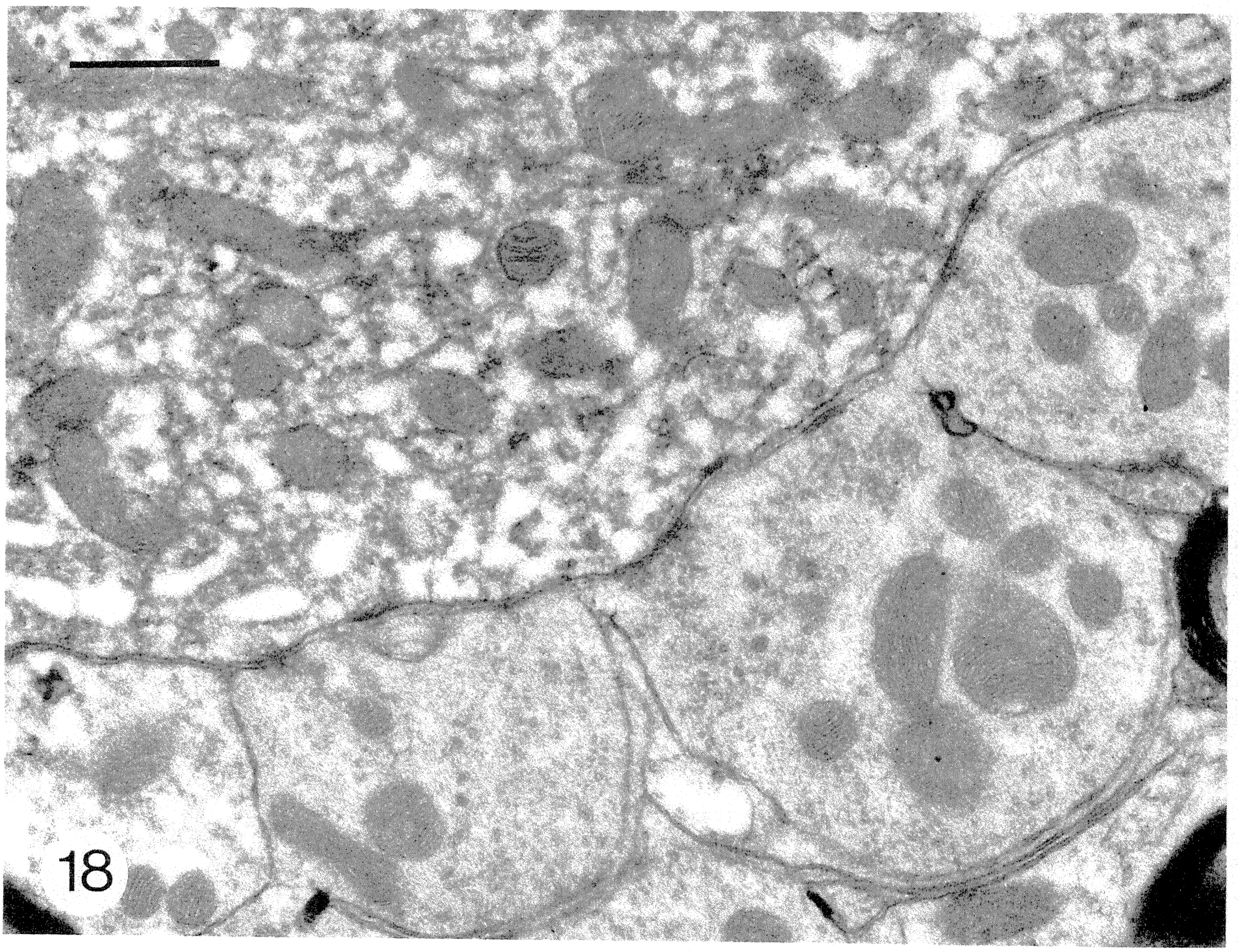

Figs. 17, 18. Electron micrographs of a glutamate-positive large fusiform ELL neuron that is densely covered with synaptic boutons. Figure 18 is a detail of Figure 17 showing the structure and synaptic specializations of some of the boutons contacting a glutamate-positive large fusiform cell. Scale bars = 2 μm in Figure 17, 0.5 μm in Figure 18.

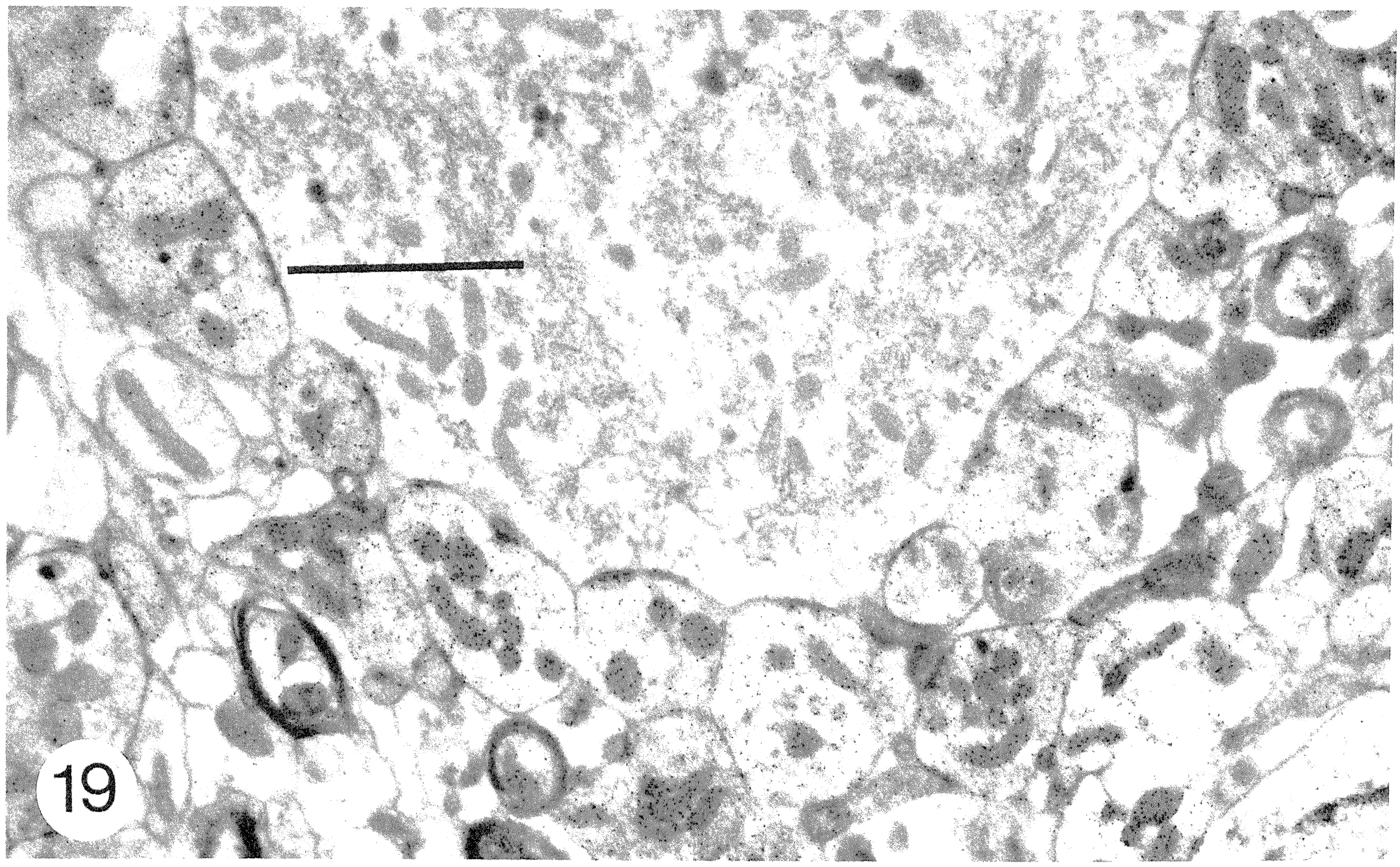

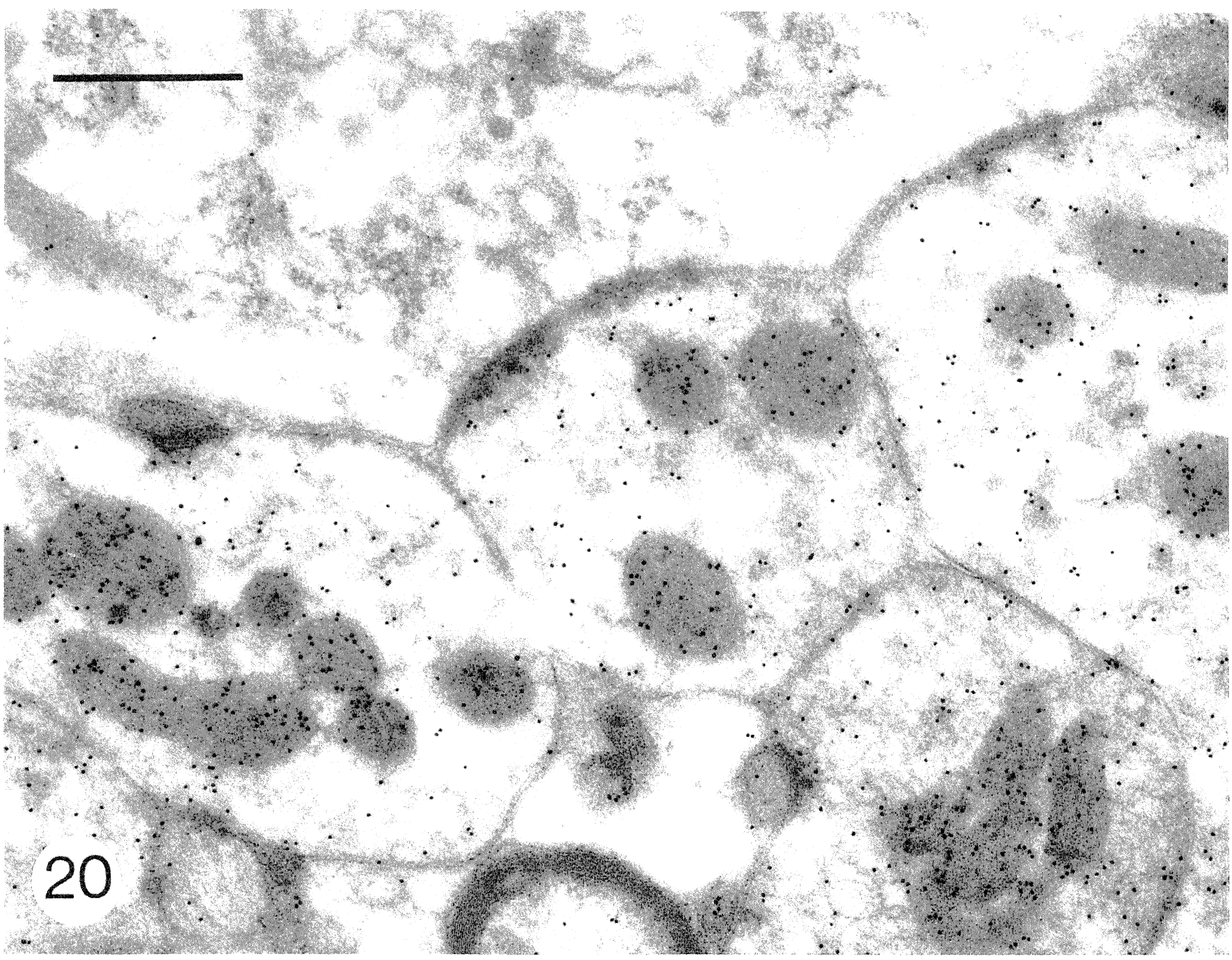

Figs. 19, 20. Electron micrographs of a lowicryl-embedded section of the mormyrid ELL treated for postembedding GABA immunohistochemistry showing the basal part of a large (GABA-negative) fusiform cell that is densely covered with GABA-positive terminals. Figure 20 is a detail of Figure 19 showing GABA-positive boutons that make synaptic contact with the GABA-negative large fusiform cell at high magnification. Scale bars = 2 μm in Figure 19, 0.5 μm in Figure 20.

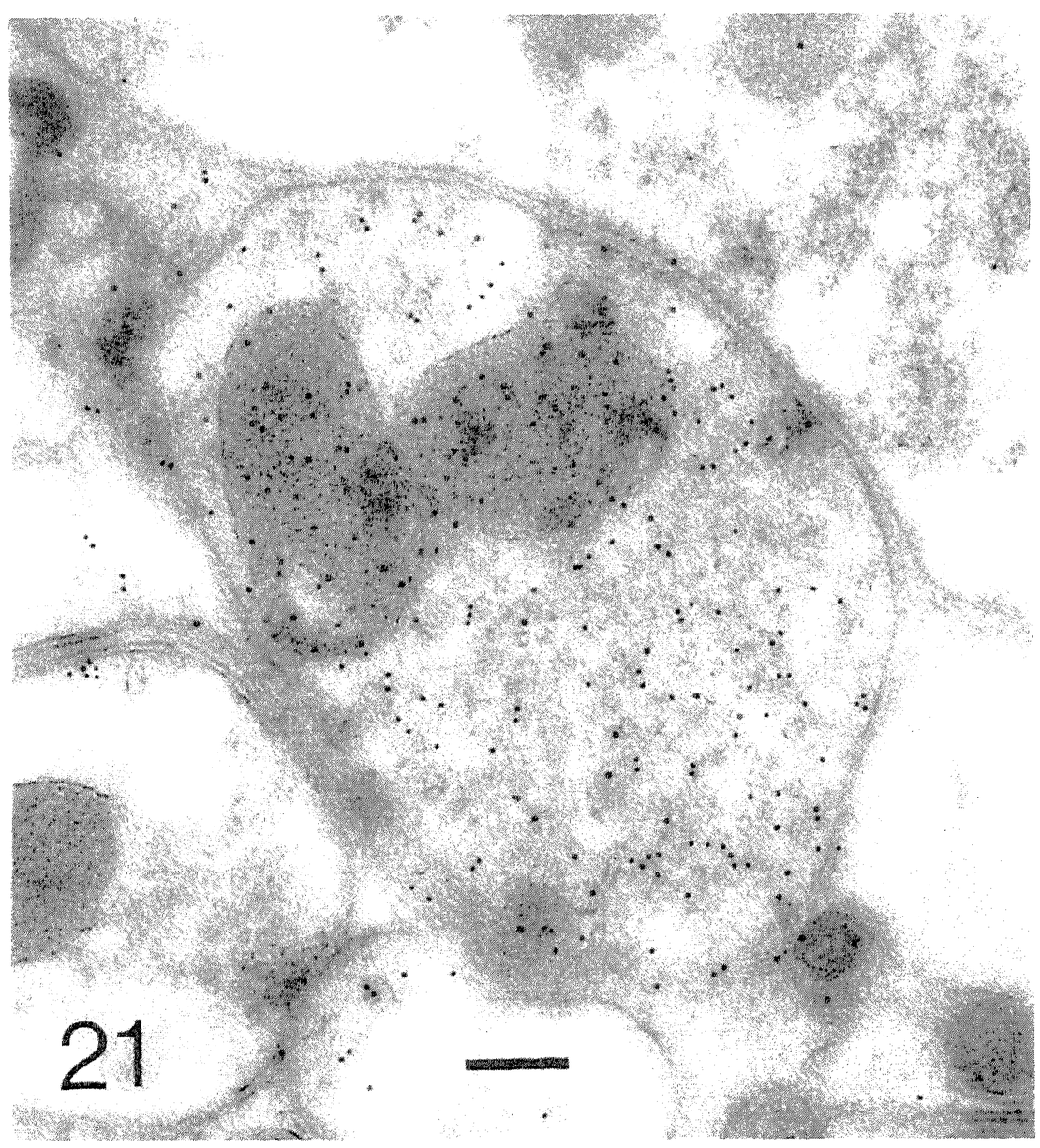

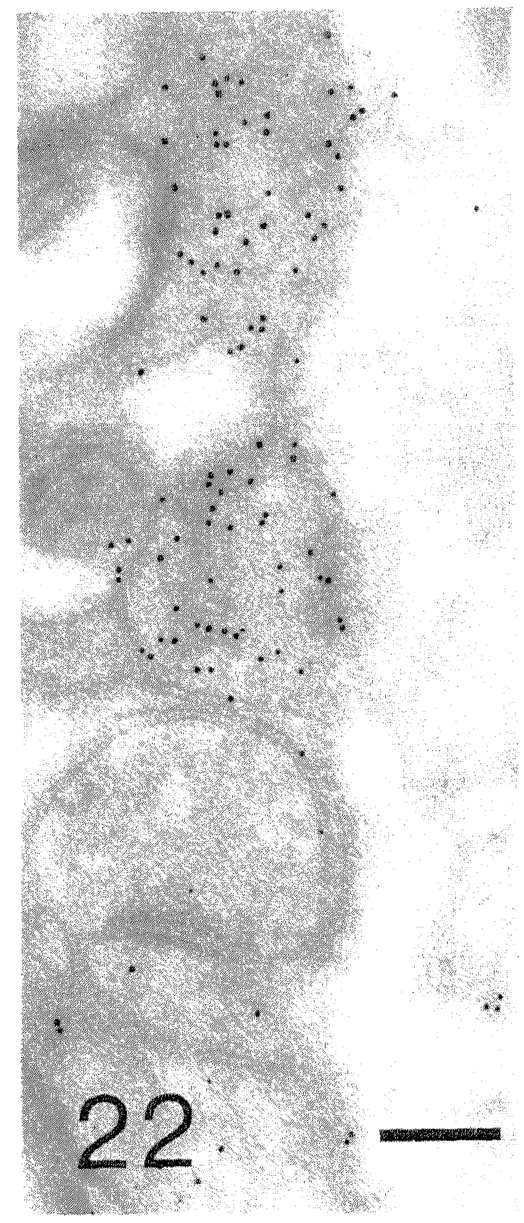

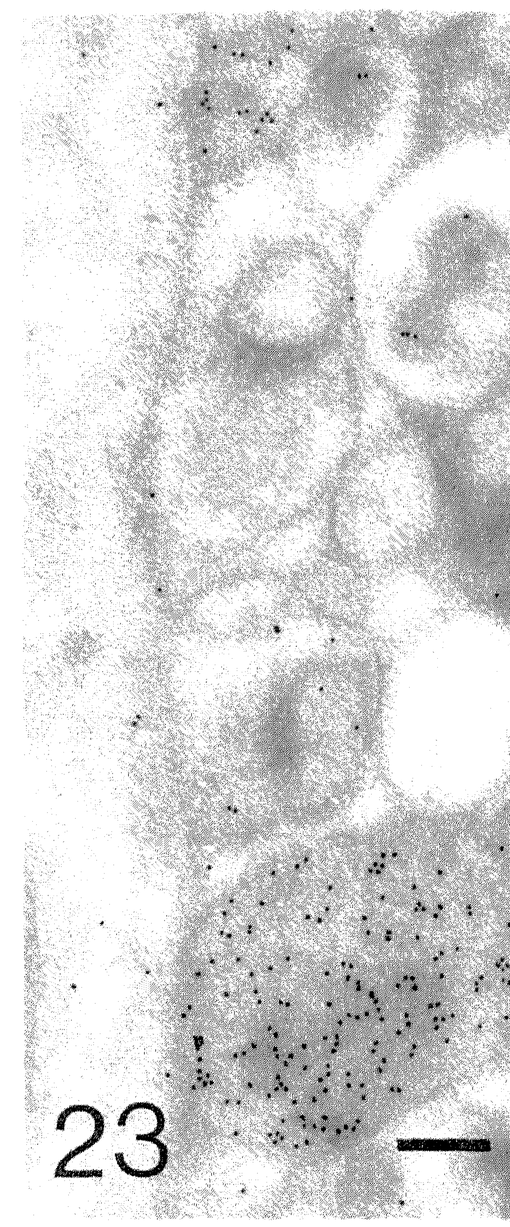

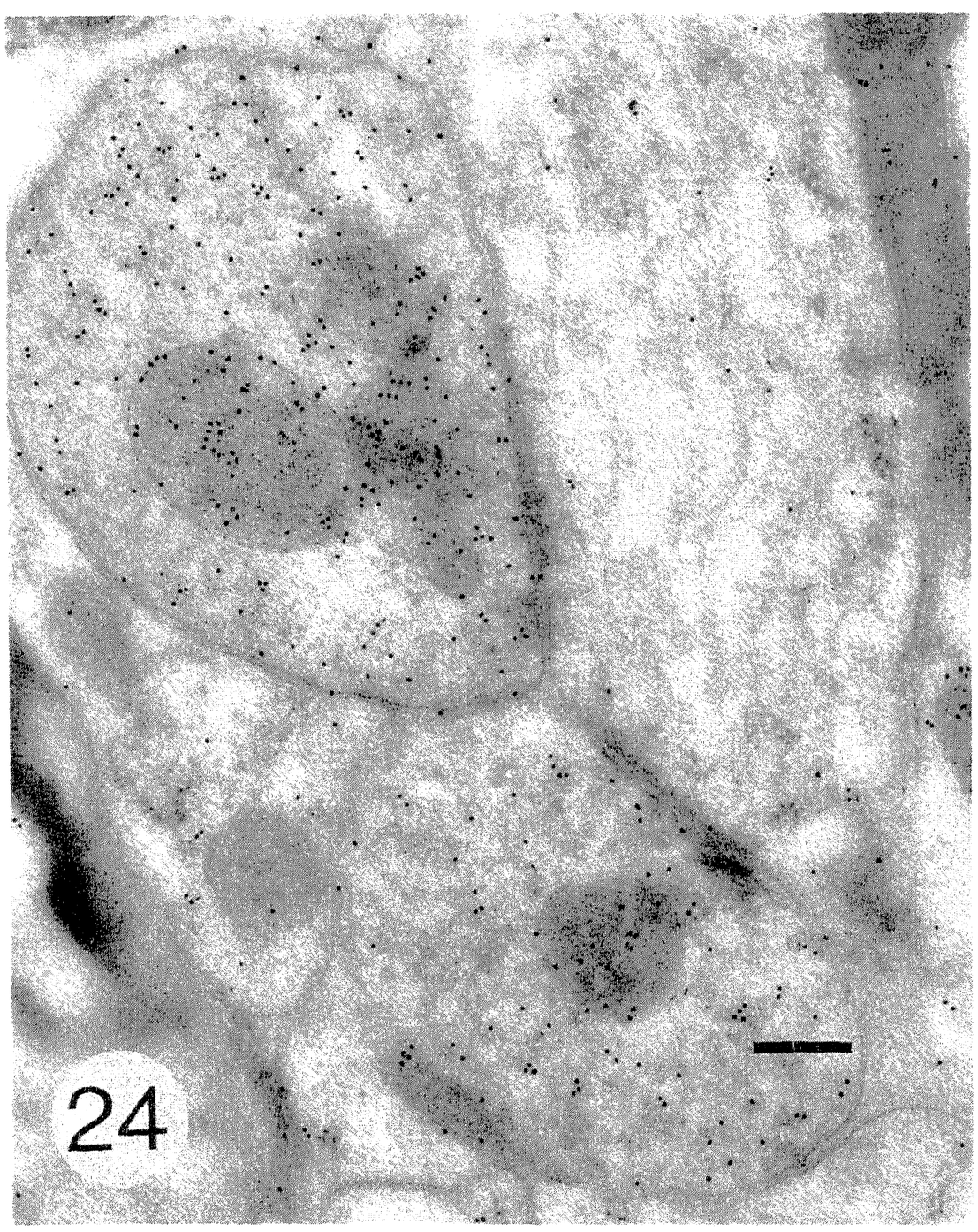

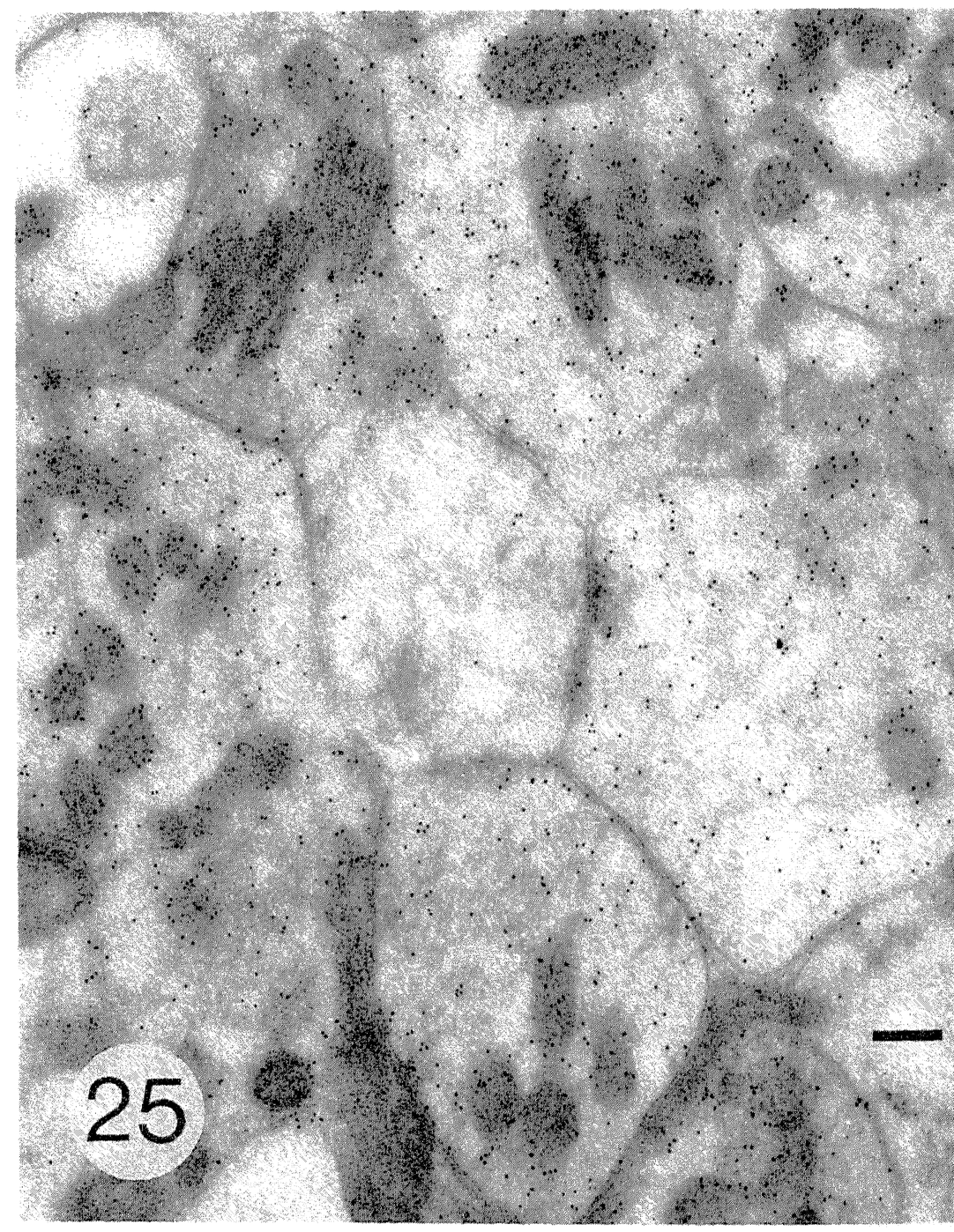

Figs. 21–25. Details of synaptic contacts of large ganglionic or large fusiform cells observed in lowicryl-embedded ultrathin sections treated for postembedding GABA immunohistochemistry. Figure 21 shows an electron micrograph of a GABA-positive terminal making synaptic contact with the cell body of a GABA-negative large ganglionic cell. Scale bar = 0.2 μm. Figures 22 and 23 are electron micrographs of GABA-negative spiny dendrites in the ELL molecular layer with GABA-negative presynaptic elements contacting spines and GABA-positive presynaptic elements contacting the smooth dendritic shaft. Figures 24 and 25 are longitudinal (Fig. 24) and transverse (Fig. 25) views of two presumed basal dendrites of large ganglionic cells that are densely covered with GABA-positive synaptic boutons. Scale bars = 0.2 μm.

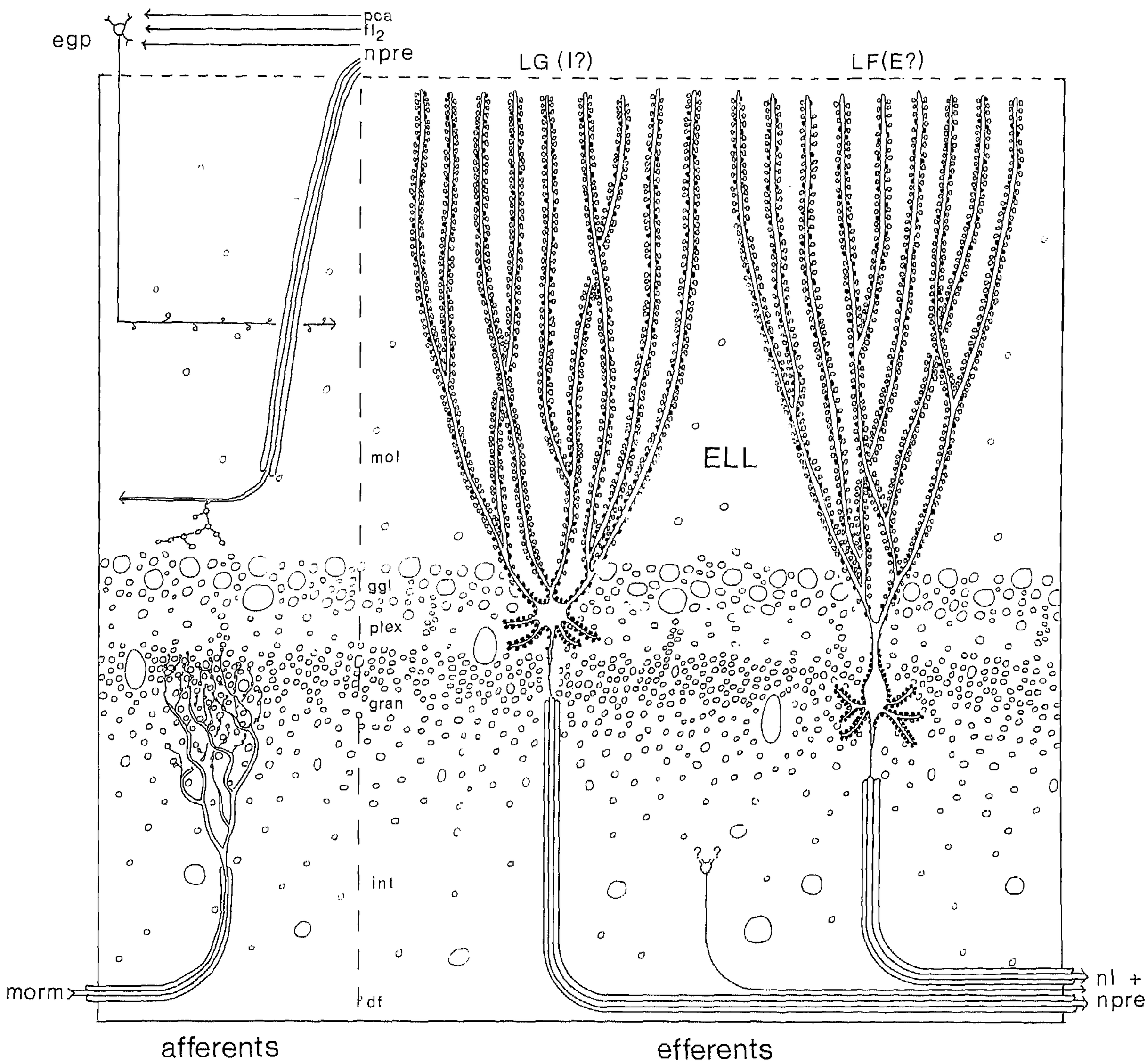

Fig. 26. Summary drawing of the present findings concerning the projection neurons of the mormyrid ELL (right) and the distribution of afferents arising from mormyromasts (morm), from the posterior granular eminence (egp), and from the preeminential nucleus (npre), as reported in the literature (for references, see text). Soma size, dendritic length, extension and number as well as synaptic contact numbers have been drawn to scale; each synaptic contact and each spine drawn, in fact, represents ten synaptic contacts or spines, respectively. Excitatory axonal terminals and cells have been drawn in white, and inhibitory synaptic contacts have been drawn in black. The background circles represent a schematic Nissl picture of the ELL layers. Myelinated axons are indicated by four parallel lines, indicating a central axon surrounded by a myelin sheath. Possible ways in which afferents may influence the efferents are presented in the Discussion. LG, large ganglionic cells; I, I units; LF, large fusiform cells; E, E units.

Intracellular in vitro dye injections show that most LG and LF cells have apical dendrites spanning the complete deep-to-superficial extent of the molecular layer (Fig. 26) but that some have a dendritic arborization that is restricted to the deeper part of the molecular layer (Fig. 6). Are these neurons with shorter apical dendrites a separate population, or were they simply damaged in some way, preventing complete filling of the dendritic arborization? The intracellular fills were made in 400-μm-thick slices and, whereas dendrites reaching the slice surface may have been truncated, those in the center of the slice were expected to be intact. It was a remarkable general property of projection neurons that, for any given labeled cell, the large majority of all the apical dendrites terminated within the slice, and these were all approximately the same length. Consequently, we believe that a certain percentage of LG and LF cells do indeed have dendrites restricted to the deep molecular layer. A possible interpretation is that cells with short apical dendrites are growing cells, because most short dendrites have tips ending in a growth cone-like structure.

Different cells have dendrites terminating at different heights in the molecular layer, probably representing different stages of cellular growth. In addition, cells with short apical dendrites have variable apical dendritic diameters, also suggesting developmental processes. Finally, other cell types in the ganglionic layer, which are described in the accompanying paper (Meek et al. 1996), show the same phenomenon, which is correlated clearly with a smaller soma size, fewer dendrites, and a lower spine density, all suggesting a developmental process.

Fish brains are peculiar, because they grow throughout life like the rest of the body, even when the fish are sexually mature, as has recently been demonstrated experimentally for gymnotid fish by Zupanc and Horschke (1995). The fish used in the present experiments (10–15 cm) were still growing, because large specimens may reach a length of 25–30 cm. Thus, the volume of the ELL must increase substantially with body size, and the addition of new cells seems to be a continuous process involved in such growth (Zupanc and Horschke, 1995). Whether the response properties of LG and LF with short dendrites are similar to those of (mature) cells with long dendrites is unknown at present, as is the ratio and frequency of occurrence of presumed growing LG and LF cells.

To evaluate the significance of the present findings, as summarized in Figure 26, we will compare them below with previous morphological and physiological studies on the mormyrid ELL and cerebellum and with the organization of homologous lobes or regions in gymnotid electric fish and some other, nonelectric teleosts.

Comparison with previous morphological studies on the mormyrid ELL

Previous studies of the morphological features of the mormyrid ELL (Maler, 1973; Maler et al., 1973a,b; Bell and Russell, 1978; Bell et al., 1981, 1989) used a different delineation of the granular and intermediate layers. These authors distinguished a rather narrow (30 μm) granular layer and a very broad (150 μm) intermediate layer, subdivided into a superficial part (approximately 75 μm) with an approximately equal density of small cells and fibers, and a deep part dominated by thick myelinated fibers, with a few interspersed small and large neurons (Fig. 1). Consequently, there are, in fact, three layers with quite different properties, and perhaps the introduction of a new name for the old superficial intermediate layer would be the best solution. However, a subdivision of the ELL into six layers and the correlated nomenclature have already been accepted for some time, and it seems most useful to adopt and maintain this. Within this framework, we prefer to include the old superficial intermediate layer in the granular layer for the following reasons.

In Kluver-Barrera stained and plastic-embedded semithin sections (Fig. 1C,D), it is obvious that there is a sharp transition in myelin density between the old superficial and deep intermediate layers; this indicates a crucial difference. Such a difference is not present between the old superficial intermediate and granular layers, where only a gradual increase in the density of granule cells can be observed (Figs. 1A,B,D, 26). Consequently, it seems more appropriate to include the old superficial intermediate layer in the granular layer, because this unequivocally refers to the most characteristic property of this (sub)layer: the presence of large numbers of granule cells. Moreover, it appears that primary afferents terminate exclusively in the (new) granule layer and that LF cells occur throughout the (new, superficial as well as deep) granule layer, whereas multipolar intrazonal neurons (Meek et al., 1994), for example, occur exclusively in the (new) intermediate layer. A distinction between superficial and deep granular layers is still necessary, however, because the density of granular elements is different in these sublayers; because their immunohistochemical properties, as visualized with antibodies against Calbindin proteins, are different (Bell, personal communication); and because a population of very small neuronal or glial cells is particularly dense in the (new) superficial granular layer (Fig. 1C).

Previous studies on the morphological characteristics of mormyrid ELL projection neurons are very limited, whereas studies on their synaptology and immunohistochemistry are completely lacking. In, 1973, Maler published a Golgi study of the mormyrid ELL in which he described the presence of large beard cells in the superficial granular layer that are clearly those described here as LF cells. However, we found a broader distribution of their location than Maler (1973), because, in the present study, LF cells were found in both the superficial and the deep granular layers, whereas Maler described beard cells only in the superficial granule layer. LG cells were apparently not impregnated in the material of Maler (1973) and, consequently, could not be described at that time. However, the retrograde labeling experiments of Bell et al. (1981) clearly showed their existence as well as the presence of small projection neurons in the intermediate layer.

The projection neurons described in the present paper are the final common output pathway of the mormyrid ELL, relaying a variety of processed and integrated inputs to targets in the isthmus region and the midbrain. The most important inputs to the ELL are summarized in Figure 26 and include primary afferents, preeminential afferents, and parallel fibers from the eminentia granularis posterior (egp). Primary afferents from mormyromast electroreceptors terminate exclusively in the superficial and deep granular layers (Bell et al., 1989; present study). Preeminential fibers terminate exclusively in the deep part of the molecular layer (Bell et al., 1981), whereas the parallel fibers in the remaining part of the molecular layer all seem to originate from the egp (Maler, 1973, 1974; personal observations). At present, it is supposed that primary afferents (Bell, 1990a,b), parallel fibers (Bell et al., 1992), and preeminential afferents (unpublished observations; see also Meek, 1993, 1994) all have excitatory effects on their targets. In addition to these main ELL inputs, serotonergic fibers arising from raphe nuclei (Grant et al., 1989; Meek and Joosten, 1989), noradrenergic fibers from the locus coeruleus or a caudal rhombencephalon cell group (Meek et al., 1993), and juxtalobar afferents, arising from a (juxtalobar) nucleus involved in the corollary electromotor command circuit (Bell et al., 1995) also play a role in ELL circuitry.

The precise pathways and circuits by which ELL inputs are processed and reach the ELL projection neurons are still largely unknown. It is fairly well established that the majority of the input to the spiny apical dendrites of LG and LF cells arises from the egp, which relays integrated proprioceptive, preeminential (i.e., electrosensory as well as command-associated input), and paratrigeminal command-associated input (Bell et al., 1992; see Fig. 26) directly to the ELL projection neurons. However, several indirect pathways between egp parallel fibers and LG as well as LF cells

that are mediated by interneurons also exist (see Meek et al., 1996). The existence of direct connections between preeminential afferents and LG or LF cells is not yet certain. Preeminential afferents terminate predominantly on spines in the deep molecular layer (Meek, 1993), but it is unknown whether these belong to LG, LF, or other types of ganglionic cells with spiny dendrites in the molecular layer (see Meek et al., 1996).

The microcircuitry by which primary afferent input reaches ELL projection cells is still unknown. Primary afferents terminate predominantly on small dendrites and on small neurons in the granular layer, where they make predominantly asymmetric chemical synapses and some mixed synapses, consisting of a chemical synapse and a gap junction (Bell et al., 1989). Direct contacts on LF cells were not described by Bell et al. (1989), despite the fact that the somata and basal dendrites of LF cells are located within the terminal fields of primary afferents. The present study tends to confirm the absence of direct contacts between primary afferents and LF cells, because very few non-GABAergic synaptic contacts were found on the surfaces of their somata and proximal dendrites, whereas the few possible examples that were observed did not resemble primary afferent terminals, as described previously (Bell et al., 1989). Thus, the suggestion that the different locations of LG and LF cells are correlated with the absence or presence of direct synaptic input from primary afferents is not confirmed by the present analysis of their synaptic input. Although it remains possible that distal parts of basilar dendrites of LF cells, which could not be identified and analyzed in the EM in the present study, receive some direct primary afferent input, it is most likely that all contacts between primary afferents and ELL efferent neurons are mediated by granular cells. Further analysis is necessary to determine which granular cell types are involved and whether similar or different types of granule cells relay primary afferent input to LG and LF cells. The different locations and distributions of both LG and LF cells as well as the fact that LG cells are probably inhibited by primary afferent input, whereas LF cells are probably excited by primary afferent input (see below), suggest that different types of granular cells, or at least different granular layer circuits, are intercalated between primary afferent input and LG or LF cells.

Comparison with physiological data

Several physiological studies have described the interactions of electrosensory input and corollary electromotor command-associated input to the ELL (for review, see Bell, 1986, 1989). In the mormyromast zones of the ELL, electrosensory input arrives in the granular layer and produces receptive fields with a strong center surround, or lateral inhibition (Bell et al., 1989; Bell, 1990a). An important source of corollary command-associated input to the ELL is the egp, which projects to the molecular layer, forming the parallel fibers that run at right angles to the apical dendrites of LG and LF neurons (Bell et al., 1992). LF cells seem to be in an optimal position to integrate these electrosensory and electromotor command-associated signals, because they receive input in both the molecular layer and the granular layer. However, the situation seems more complicated than was previously thought, because a recent work (Bell et al., 1995) shows that command-associated input also appears to be relayed to the granular and plexiform layers via the juxtalobar nucleus. LG cells are in an optimal position to integrate such juxtalobar command-associated input to the plexiform layer with molecular layer input.

Extracellular recordings have shown that single units in the mormyromast region of the ELL can be subdivided into two populations: E units, which are excited in the center of their receptive field by primary afferent input, and I units, which are inhibited by similar input. I units are concentrated in the ganglionic layer (Bell and Grant, 1992), suggesting that they might well include LG cells. On the basis of the responses to electromotor command corollary discharges, three subtypes of I units can be distinguished: I_1 with a stereotyped, short latency effect of corollary discharges; I_2 with a stereotyped, but weaker effect at a longer latency; and I_3, with rather weak and plastic effects of electromotor command-associated input (Bell and Grant, 1992). To investigate which of the response properties belong to LG cells and which belong to ganglionic layer interneurons, whose morphology and synaptology are described by Meek et al. (1996) in the accompanying paper, it will be necessary to combine intracellular recording and labelling in vivo.

E units can be found in the ganglionic, plexiform, and granular layers (Bell and Grant, 1992), which strongly suggest that they include LF cells. The somata of LF neurons are distributed throughout the deep and superficial granular layer, whereas their large-diameter, proximal apical dendrites traverse the plexiform and ganglionic layers. The location of their cell bodies within the terminal fields of primary afferents is in accordance with expected E responses, but, as has already been discussed, evidence for direct contacts between primary afferents and LF cells is still lacking. Preliminary results obtained from in vivo intracellular labeling of ELL units tend to confirm the conclusion that LG cells are I units and that LF cells are E units (Bell, personal communication). E cells show heterogeneous and plastic interactions of electrosensory and electromotor corollary discharge input (Bell and Grant, 1992; Bell, 1993; Bell et al., 1993), but the underlying circuitry is unknown at present.

Comparison with the cerebellum

The ELL combines a number of cortical characteristics with certain cerebellar features. Cortical characteristics include the presence of several layers with a topographical organization, as encountered in the mammalian neocortex, but also, for example, in the teleostean tectum (Meek, 1983) and the gymnotid ELL and midbrain torus semicircularis (for review, see Carr and Maler, 1986). The significance of these organizational aspects is evaluated in the accompanying paper (Meek et al., 1996). Cerebellar aspects of the mormyrid ELL include the presence of a large molecular layer with numerous transversely running parallel fibers, terminating on the spines of dendrites of large, more deeply located cells. Comparison of these features with those encountered in the mormyrid cerebellum (as studied by Meek and Nieuwenhuys, 1991; Meek, 1992a,b) reveals the following interesting similarities and differences.

In contrast to cerebellar organization, the parallel fibers in the ELL molecular layer originate from outside the ELL, i.e., from the cerebellar posterior granular eminences. This has already been described by Maler (1973, 1974) and has been confirmed by our own recent Golgi impregnations and tracing experiments (Grant and Meek, unpublished observations). This is correlated with the fact that the ELL

originates phylogenetically from the cerebellar crest and the underlying medial octavolateral nucleus (see below). Maler's suggestion (Maler, 1973) that some parallel fibers might originate from ELL granule cells has not been confirmed in the present study. Consequently, we assume that probably all, and at least the majority, of the parallel fibers in the mormyrid ELL originate from the egp. However, the precise origin within egp and the distribution of parallel fibers in different ELL zones and regions require further study.

The superficial origin of parallel fibers in the mormyrid ELL molecular layer adds a new configuration to the different possibilities encountered in the mormyrid brain. It has been shown that parallel fibers in the mormyrid cerebellum originate not only from granule cells located in a layer below the layer of Purkinje cells but also at several sites within granule cell masses located unilaterally (e.g., in the valvula) or bilaterally (e.g., in the lobus transitorius) to the molecular layer (Meek, 1992a,b). It has been postulated that such configurations are involved specifically in the detection of temporal differences in input by means of coincidence detection (Meek, 1992a,b). The ELL molecular layer seems to present a good model to test this hypothesis. In particular, the differences between the MZ and the DLZ are interesting in this respect. In the DLZ, the granule cells of egp are located immediately above the molecular layer and penetrate the molecular layer vertically, after which they turn horizontally (or bifurcate) to take a course parallel to the deeper layers. However, in the MZ, parallel fibers penetrate the molecular layer laterally from either side but not from a dorsal direction. Thus, the MZ molecular layer has a rather simple parallel fiber organization that could be promising for the investigation of interactions between parallel fiber activity waves arising from the left or the right granule cell masses of the egp.

Within the molecular layer, parallel fibers terminate on spines of large deep cells, a situation similar to the cerebellum. We estimated a number of about 10,000 spines per large projection cell, a number comparable to that calculated for mormyrid Purkinje cells (Meek and Nieuwenhuys, 1991). Moreover, the smooth surface of the spiny dendrites is contacted by inhibitory synaptic terminals, probably arising from stellate cells (Meek et al., 1996), a situation also resembling that of Purkinje cells. Thus, the intrinsic organization of the molecular layer of the ELL is quite similar to the intrinsic organization of the cerebellar molecular layer.

A major difference between the ELL and the cerebellar molecular layer is the fact that the spiny dendrites originate from different cells: In the cerebellum, they belong to Purkinje cells, and, in the ELL, they belong to both LG and LF cells and to ganglionic interneurons (Meek et al., 1996). Comparison of Purkinje cells with LG and LF cells reveals several particular differences. A first important difference is that LG and LF cells are not oriented in a sagittal plane to the same extent as Purkinje cells; moreover, the latter form a striking palisade pattern in the mormyrid cerebellum (Meek and Nieuwenhuys, 1991). The significance of this difference is uncertain, but the more random orientation of LG and LF dendritic trees suggests that their role is not a very precise encoding of the temporal aspects of parallel fiber input, as is presumed for Purkinje cells (Meek, 1992a). A second difference concerns the position of Purkinje cells and LG and LF cells in the circuitry of the cerebellum and ELL, respectively. Purkinje cells are interneurons (Meek and Nieuwenhuys, 1991) that use GABA as a neurotransmitter (Meek, unpublished observations), whereas LG and LF cells are projection neurons that use glutamate as a transmitter. Moreover, mormyrid Purkinje cells express the cerebellar peptide zebrin-II, whereas ELL cells, including LG and LF cells, do not (Meek et al., 1992). In this respect, LG and LF cells are more similar to cerebellar eurydendroid cells, the teleostean cerebellar output elements (see, e.g., Nieuwenhuys and Nicholson, 1969; Nieuwenhuys et al., 1974; Meek et al., 1986a,b; Ito and Yoshimoto, 1990) than to Purkinje cells. However, cerebellar eurydendroid neurons have smooth dendrites in the cerebellar molecular layer (Nieuwenhuys et al., 1974; Ito and Yoshimoto, 1990), whereas LG and LF cells have spiny apical dendrites.

A characteristic feature of cerebellar Purkinje cells is their dual input from parallel and climbing fibers. The latter arise from the inferior olive (for review, see Ito, 1984). In teleosts, climbing fibers terminate preferentially on the proximal parts of the apical dendrites of Purkinje cells (Pouwels, 1978a,b; Meek and Nieuwenhuys, 1991; Meek, 1992b). The ELL has no climbing fiber input from the inferior olive (Bell et al., 1981; Bell and Szabo, 1986). Instead, LG and LF cells probably receive input from the preeminential nucleus to their proximal dendrites. Labelling with tracers has shown that preeminential axons terminate in the deep molecular layer (Bell et al., 1981) immediately above the ganglionic cell layer, predominantly on dendritic spines (Meek, 1993; unpublished observations). Thus, it is plausible to assume that, although it has not yet been unequivocally demonstrated, these synaptic sites include spines of LG and LF cells. Consequently, preeminential input to LG and LF cells and climbing fiber input to mormyrid Purkinje cells, as described by Meek and Nieuwenhuys (1991), show several striking similarities: They both terminate with asymmetric (therefore, probably excitatory) synaptic terminals on spines located on the most proximal part of the spiny apical dendrites. This suggests that preeminential input to the ELL might have a function similar to that of climbing fiber input to the cerebellum in the interaction with and possibly "instruction of" parallel fiber input (see, e.g., Ito, 1984). Plastic changes in responsiveness of ELL neurons to parallel fiber input are strongly suggested by the results of Bell et al. (1993) and of Bell (1993), and the role of preeminential fiber input in this respect is an interesting topic for further study and for comparison with cerebellar functional plasticity.

Comparison with gymnotids

Mormyrids are not the only group of active electrosensory teleosts. Gymnotids also have an electric organ and electroreceptors, which they use for electrocommunication as well as for active electrolocation (Bullock et al., 1983; Bell; 1986; Carr and Maler, 1986). Interestingly, the African mormyrids and American gymnotids have developed their electrosensory capacities independently during phylogeny (Bullock et al., 1983), and comparison of the two groups yields interesting examples of the constraints and variabilities involved in the convergent evolution of this sensory capacity.

The morphological organization of the gymnotid ELL has been investigated in detail (Maler, 1979; Maler et al., 1981, 1982; Carr et al., 1982; Carr and Maler, 1986; Mathieson et al., 1987; Maler and Mugnaini, 1994) and bears a striking resemblance to the organization of the mormyrid ELL. Most of the six layers are known by similar names in the

two species, whereas the mormyrid ganglionic layer is very similar to the gymnotid pyramidal cell layer, and the mormyrid intermediate (cell and fiber) layer corresponds to the gymnotid deep neuropil layer. A minor difference concerns the location of preeminential afferents in the two groups. Although these afferents terminate in the deep molecular layer in both groups, they reach this region by a different route: In gymnotids, they establish a tract of myelinated fibers between the molecular and pyramidal layer, known as the striatum fibrosum (Maler, 1979; Maler et al., 1981), whereas, in mormyrids, they course between the egp and the molecular layer of ELL, thus, establishing a superficially located preeminential ELL tract, sometimes indicated as the peet (the preeminential-electrosensory tract; Bell et al., 1981; Bell and Szabo, 1986). The lemniscal projection neurons of the gymnotid ELL are concentrated in the pyramidal layer, where both basilar and nonbasilar pyramidal neurons are found (Maler, 1979; Maler et al., 1981). In addition, a smaller population of so-called deep basilar pyramidal projection neurons has been described with cell bodies located in the granular layer (Bastian and Courtright, 1991; Maler and Mugnaini, 1994).

There are several striking similarities between lemniscal projection cells in mormyrids and gymnotids. In both groups, these neurons have spiny apical dendrites in the molecular layer that receive excitatory input from egp parallel fibers (for gymnotids, see Maler et al., 1981) and inhibitory input from stellate cells (for gymnotids, see Maler and Mugnaini, 1994), and, in both groups, these neurons form a glutamatergic projection (for gymnotids, see Wang and Maler, 1994) to the preeminential nucleus and the midbrain torus semicircularis (for gymnotids, see Maler et al., 1982). Moreover, LG cells share with gymnotid pyramidal cells the property that their somata are located in the layer of large cells just below the molecular layer, i.e., the ganglionic layer in mormyrids and the pyramidal cell layer in gymnotids (Maler, 1979; Maler et al., 1981). In particular, LG cells resemble nonbasilar pyramidal cells, because neither type has dendritic processes in the granular layer or below; thus, they do not receive direct electrosensory input (for gymnotids, see Maler et al., 1981). In addition, it has been shown that nonbasilar pyramidal neurons are inhibited by electrosensory stimulation of the center of their receptive field (Bastian, 1981a,b), and this is also strongly suggested for LG cells (see above). The somata and basal dendrites of ganglionic or pyramidal neurons in the ganglionic, pyramidal, or plexiform layers receive exclusively inhibitory GABAergic input (for gymnotids, see Maler and Mugnaini, 1994).

Mormyrid LF cells resemble gymnotid basilar and deep basilar pyramidal cells, in that they have E-type responses to electrosensory input (for gymnotids, see above; Bastian, 1981a,b; Bastian and Courtright, 1991). In gymnotids, this is correlated with the presence of the basal dendrite, which receives direct primary electrosensory input in the granular and deep neuropil layer (Maler et al., 1981; Mathieson et al., 1987). LF cells differ substantially from basilar pyramidal neurons in this respect: They have no long, vertically oriented basilar processes in the granule and/or intermediate layer; instead, they have a cell body with short basal dendrites in the granule layer that may not receive any direct electrosensory input.

Mormyrid LF cells resemble gymnotid deep basilar pyramidal cells, in that they have a cell body in the granular layer and apical dendrites in the molecular layer. However, the apical dendrites of deep basilar pyramidal cells are short and restricted to the ventral (deep) molecular layer (Bastian and Courtright, 1991). Similar cells have been observed in mormyrids (e.g., Fig. 6f), but we presume that these are growing cells (see above). In gymnotids, this does not seem to be the case, because tracer labelling shows that, unlike more superficial basilar pyramidal neurons, deep basilar pyramidal neurons project exclusively to the preeminential nucleus (Bastian and Courtright, 1991). This points to the possibility that, in mormyrids, there may also be some projection cells that project only to the preeminential nucleus and not to the lateral toral nucleus, although such a population is not described in the present paper. Retrograde tracing from the nucleus preeminentialis will be used to resolve this question in the future.

Comparison with other teleosts

McCormick (1982, 1983) pointed out that the ELL of electrosensory teleosts should be considered as a lateral extension of the mechanosensory lateral line (or medial octavolateral) nucleus of the teleostean rhombencephalon. The phylogenetic development of this lobe seems to have occurred independently for the two groups of passive electrosensory teleosts, i.e., the *Ictaluridae* and *Xenomystinae*, as well as for the active electrosensory Gymnotidae and Mormyridae (McCormick, 1982; Bullock et al., 1983; Finger et al., 1986). Comparison of the organization of the mormyrid ELL with that of passive electrosensory teleosts as well as with that of the teleostean mechanosensory lateral line region, consequently, is useful for tracing back some of the possible evolutionary processes that might have been involved in the development of these huge and highly differentiated structures.

The mechanosensory lateral line region of the brain of teleosts consists of the medial octavolateral nucleus covered by the cerebellar crest (see McCormick, 1982, 1983). The cerebellar crest is a (molecular) layer of parallel fibers originating from the caudal cerebellar granular eminences (Larsell, 1967; Maler, 1974). These parallel fibers terminate with asymmetrical synaptic contacts on the spiny dendrites of so-called crest cells (Diaz-Reguera and Anadon, 1995), which are the projection neurons of the medial octavolateral nucleus (Finger and Tong, 1984; McCormick, 1983). The morphology of teleostean crest cells has been described in most detail by Meredith (1984) for the cichlid fish *Astronotus*, in which neurons both with and without basal dendrites occur, similar to the situation in the ELL of gymnotids. Below the layer of crest cells, smaller granular or polygonal cells occur, which are the main recipients of primary mechanosensory input (Caird, 1978; Finger and Tong, 1984; Meredith, 1984).

Comparison of the mormyrid ELL projection neurons with the mechanosensory teleostean crest cells shows the same differences and similarities as comparison with the gymnotid ELL pyramidal cells. Similarities include the presence of spiny apical dendrites, a large soma in the boundary region between the cerebellar crest (or molecular layer) and the deeper located medial nucleus (or ELL layers), and the presence of short basal dendrites. Differences include the presence of crest cells with long basal dendrites, which are absent in mormyrids. Instead, mormyrids have deeper located large fusiform cells, for which no homologue has been observed in the teleostean mechanosensory lateral line region. Thus, it is uncertain whether LF neurons represent a kind of displaced crest cell with a

function similar to that of crest cells with basal dendrites or whether they are a cell type that evolved from the deeper population of polygonal and granule cells of the mechanosensory lateral line region. Another uncertainty concerns the transmitter used by crest cells: Whereas it is clear in gymnotids and mormyrids that the pyramidal ganglionic and fusiform projection cells use glutamate as a neurotransmitter, this is uncertain for teleostean crest cells. A curious observation in this respect is that many crest cells of the mormyrid mechanosensory lateral line lobe, the homologue of the medial octavolateral nucleus of other teleosts, are GABAergic (Meek, unpublished observations). Whether this also holds true for the lateral line region of other teleosts or is a mormyrid specialization is presently unknown. It is also unknown whether the GABAergic crest cells of the mormyrid mechanosensory lateral line lobe are projection neurons or interneurons and whether non-GABAergic crest cells also occur in this lobe.

The cell types and some synaptic connections of the ELL of the passive electrosensory catfish *Ictalurus* have been described by Finger (1986), who showed that the organization of this ELL has a complexity that is intermediate between the mechanosensory lateral line region and the gymnotid ELL. Similar to the latter structures, the ELL of *Ictalurus* contains crest cells without (type I) and with (type II) basal dendrites, giving I- and E-type responses, respectively, the latter of which are mediated by direct synaptic contacts between primary electrosensory afferents and the basal dendrites of type II crest cells (Finger, 1986). The latter, as discussed above, have not been observed in the mormyrid ELL. In conclusion, the structure of the mormyrid ELL seems to deviate from the general developmental trend shown by comparison of the teleostean mechanosensory lateral line region with the ELL of the passive electrosensory catfish and the gymnotid ELL. This deviation is greatly strengthened if the comparison is extended to include interneurons of the mormyrid ELL. The accompanying paper shows that the mormyrid ELL contains a large population of GABAergic ganglionic (i.e., crest cell layer) interneurons that has not been observed in the mechanosensory or ELL regions of other teleosts (Meek et al., 1996).

ACKNOWLEDGMENTS

We thank Curtis Bell for his continuous encouragement of our research and for the many stimulating discussions on ELL circuitry. We are grateful to Helmy Mulders and Henk Joosten for participation in some of the intracellular labeling and neuronal tracer experiments, respectively. We are indebted to Drs. Tappaz and Buijs for their gifts of anti-GAD and anti-GABA antibodies, respectively, and we wish to thank Ms. Inge Eijkhout for typing the paper and for secretarial assistance. This research was supported by European Science Foundation twinning grant 8906 and by a grant from the European Commission (CII*-CT92-0085) to K. Grant.

LITERATURE CITED

Abercrombie, M. (1946) Estimation of nuclear population from microtome sections. Anat. Rec. *94:*239–247.

Bass, A.H. (1986) Electric organs revisited. Evolution of a vertebrate communication and orientation organ. In T.H. Bullock and W. Heiligenberg (eds): Electroreception. New York: John Wiley and Sons, pp. 13—70.

Bastian, J. (1981a) Electrolocation I. How the electroreceptors of *Apteronotus albifrons* code for moving objects and other electrical stimuli. J. Comp. Physiol. *144:*465–179.

Bastian, J. (1981b) Electrolocation II. The effects of moving objects and other electrical stimuli on the activities of two categories of posterior lateral line lobe cells in *Apteronotus albifrons*. J. Comp. Physiol. *144:*481–494.

Bastian, J. (1986a) Gain control in the electrosensory system mediated by descending inputs to the electrosensory lateral line lobe. J. Neurosci. *6:*553–562.

Bastian, J. (1986b) Gain control in the electrosensory system: A role for the descending projections to the electrosensory lateral line lobe. J. Comp. Physiol. A *158:*505–515.

Bastian, J., and J. Courtright (1991) Morphological correlates of pyramidal cell adaptation rate in the electrosensory lateral line lobe of weakly electric fish. J. Comp. Physiol. A *168:*393–407.

Bastian, J., J. Courtright, and J. Crawford (1993) Commissural neurons of the electrosensory lateral line lobe of *Apteronotus leptorhynchus*: Morphological and physiological characteristics. J. Comp. Physiol. A *173:*257–274.

Bell, C.C. (1986) Electroreception in mormyrid fish: Central physiology. In T.H. Bullock and W. Heiligenberg (eds): Electroreception. New York: John Wiley and Sons, pp. 423–452.

Bell, C.C. (1989) Sensory coding and corollary discharge effects in mormyrid electric fish. J. Exp. Biol. *6:*229–253.

Bell, C.C. (1990a) Mormyromast electroreceptor organs and their afferent fibers in mormyrid fish. II. Intra-axonal recordings show initial stages of central processing. J. Neurophysiol. *63:*303–318.

Bell, C.C. (1990b) Mormyromast electroreceptor organs and their afferent fibers in mormyrid fish. III. Physiological differences between two morphological types of fibres. J. Neurophysiol. *63:*319–332.

Bell, C.C. (1993) The generation of expectations in the electrosensory lobe of mormyrid fish. J. Comp. Physiol. A *173:*677–680.

Bell, C.C., and K. Grant (1989) Corollary discharge inhibition and preservation of temporal information in a sensory nucleus of mormyrid electric fish. J. Neurosci. *9:*1029–1044.

Bell, C.C., and K. Grant (1992) Sensory processing and corollary discharge effects in mormyromast regions of mormyrid electrosensory lobe. II. Cell types and corollary discharge plasticity. J. Neurophysiol. *68:*859–875.

Bell, C.C., and C.J. Russell (1978) Termination of electroreceptor and mechanical lateral line afferents in the mormyrid acousticolateral area. J. Comp. Neurol. *182:*367–382.

Bell, C.C., and T. Szabo (1986) Central structures and pathways of the mormyrid electrosensory system. In T.H. Bullock and W. Heiligenberg (eds): Electroreception. New York: John Wiley and Sons, pp. 375–421.

Bell, C.C., T.E. Finger, and C.J. Russell (1981) Central connections of the posterior lateral line lobe in mormyrid fish. Exp. Brain Res. *42:*9–22.

Bell, C.C., S. Libouban, and T. Szabo (1983) Pathways of the electric organ discharge command and its corollary discharges in mormyrid fish. J. Comp. Neurol. *216:*327–338.

Bell, C.C., H. Zakon, and T.E. Finger (1989) Mormyromast electroreceptor organs and their afferent fibers in mormyrid fish. I. Morphology. J. Comp. Neurol. *286:*391–407.

Bell, C.C., K. Grant, and J. Serrier (1992) Sensory processing and corollary discharge effects in the mormyromast response of the mormyrid electrosensory lobe. I. Field potentials, cellular activity in associated structures. J. Neurophysiol. *68:*843–858.

Bell, C.C., A. Caputi, K. Grant, and J. Serrier (1993) Storage of a sensory pattern by anti-Hebbian synaptic plasticity in an electric fish. Proc. Natl. Acad. Sci. USA *90:*4650–4654.

Bell, C.C., K. Dunn, C. Hall, and A. Caputi (1995) Electric organ corollary discharge pathways in mormyrid fish. II. The juxtalobar nucleus. J. Comp. Physiol. A *177:*463–479.

Berod, A., M. Chat, L. Paut, and M. Tappaz (1984) Catecholaminergic and GABAergic anaotmical relationship in the rat substantia nigra, locus coeruleus, and hypothalamic median eminence: Immunocytochemical visualization of biosynthetic enzymes on serial semithin plastic-embedded sections. J. Histochem. Cytochem. *32:*1331–1338.

Blackstad, T.W. (1975) Electron microscopy of experimental axonal degeneration in photochemically modified Golgi preparations: A procedure for precise mapping of nervous connections. Brain Res. *95:*191–210.

Buijs, R.M., E.H. van Vulpen, and M. Geffard (1987) Ultrastructural localization of GABA in the supraoptic nucleus and neural lobe. Neuroscience *20:*347–355.

Buijs, R.M., C.W. Pool, J. van Heerikhuize, A.A. Sluiter, P. van der Sluis, M. Ramkema, T. van der Woude, and E. van der Beek (1989) Antibodies to small transmitter molecules and peptides: Production and application of antibodies to dopamine, serotonin, GABA, vasopressin, vasoactive intestinal peptide, neuropeptide Y, somatostatin and Substance P. Biomed. Res. *10:*213–221.

Bullock, T.H., R.G. Northcutt, and D.A. Bodznick (1982) Evolution of electroreception. Trends Neurosci. *5:*50–53.

Bullock, T.H., D.A. Bodznick, and R.G. Northcutt (1983) The phylogenetic distribution of electroreception: Evidence for convergent evolution of a primitive vertebrate sense modality. Brain. Res. Rev. *6:*2–46.

Caird, D.M. (1978) A simple cerebellar system: The lateral line lobe of the goldfish. J. Comp. Physiol. *127:*61–74.

Carr, C.E., and L. Maler (1986) Electroreception in gymnotiform fish: Central anatomy and physiology. In T.H. Bullock and W. Heiligenberg (eds): Electroreception. Wiley and Sons, New York, pp 319–374.

Carr, C.E., L. Maler, and E. Sas (1982) Peripheral organization and central projections of the electrosensory nerves in gymnotiform fish. J. Comp. Neurol. *211:*139–153.

Colonnier, M., and C. Beaulieu (1985) An empirical assessment of sterological formulae applied on the counting of synaptic disks in the cerebral cortex. J. Comp. Neurol. *230:*175–179.

Denizot, J.P., S. Clausse, K. Elekes, M. Geffard, K. Grant, S. Libouban, M. Ravaille-Veron, and T. Szabo (1987) Convergence of electrotonic club endings, GABA- and serotoninergic terminals on second order neurons of the electrosensory pathway in mormyrid fish, *Gnathonemus petersii* and *Brienomyrus niger* (teleostei). Cell. Tissue Res. *249:*301–309.

Diaz-Regueira, S.M., and R. Anadon (1995) Fine structure of the medullary lateral line area of *Chelon labrosus* (order Perciformes), a nonelectroreceptive teleost. J. Comp. Neurol. *351:*429–440.

Enger, P.S., S. Libouban, and T. Szabo (1976) Fast conducting electrosensory pathway in the mormyrid fish, *Gnathonemus petersii*. Neurosci. Lett. *2:*133–136.

Finger, T.E. (1986) Electroreception in catfish: Anatomy and electrophysiology. In T.H. Bullock and W. Heiligenberg (eds): Electroreception. New York: John Wiley and Sons, pp. 287–317.

Finger, T.E., and S.L. Tong (1984) Central organization of eight nerve and mechanosensory lateral line systems in the brainstem of ictalurid catfish. J. Comp. Neurol. *229:*129–151.

Finger, T.E., C.C. Bell, and C.J. Russell (1981) Electrosensory pathways to the valvula cerebelli in mormyrid fish. Exp. Brain Res. *42:*23–33.

Finger, T.E., C.C. Bell, and C.E. Carr (1986) Comparison among electroreceptive teleosts: Why are electrosensory systems so similar. In T.H. Bullock and W. Heiligenberg (eds): Electroreception. New York: John Wiley and Sons, pp. 465–481.

Floderus, S. (1944) Untersuchungen über den Bau der menschlichen Hypophyse mit besonderen Berücksichtigung der quantitativen mikromorphologischen Verhältnisse. Acta Pathol. Microbiol. Scand. *5:*1–26.

Gerfen, C.R., and P.E. Sawchenko (1984) An anterograde neuroanatomical tracing method that shows the detailed morphology of neurons, their axons and terminals: Immunohistochemical localization of an axonally transported plant lectin, *Phaseolus vulgaris* leuagglutinin (PHA-L). Brain Res. *290:*219–238.

Grant, K., S. Clausse, S. Libouban, and T. Szabo (1989) Serotoninergic neurons in the mormyrid brain and their projection to the preelectromotor and primary electrosensory centers: Immunohistochemical study. J. Comp. Neurol. *281:*114–128.

Heiligenberg, W., and J. Dye (1982) Labelling of electroreceptive afferents in a gymnotid fish by intracellular injection of HRP: The mystery of multiple maps. J. Comp. Physiol. *148:*287–296.

Horikawa, K., and W.E. Armstrong (1988) A versatile means of intracellular labeling: Injection of biocytin and its detection with avidin conjugates. J. Neurosci. Methods *25:*1–11.

Ito, M. (1984) The Cerebellum and Neural Control. New York: Raven Press.

Ito, H., and M. Yoshimoto (1990) Cytoarchitecture and fibre connections of the nucleus lateralis valvulae in the carp (*Cyprinus carpio*). J. Comp. Neurol. *298:*385–399.

Larsell, O. (1967) The Comparative Anatomy and Histology of the Cerebellum From Myxinoids Through Birds. J. Jansen (ed). Minneapolis: University of Minnesota Press.

Maler, L. (1973) The posterior lateral line lobe of a mormyrid fish. A Golgi study. J. Comp. Neurol. *152:*281–298.

Maler, L. (1974) The acousticolateral area of bony fishes and its cerebellar relations. Brain Behav. Evol. *10:*130–145.

Maler, L. (1979) The posterior lateral line lobe of certain gymnotid fish: Quantitative light microscopy. J. Comp. Neurol. *183:*323–364.

Maler, L., and E. Mugnaini (1994) Correlating gamma-aminobutyric acidergic circuits and sensory function in the electrosensory lateral line lobe of a gymnotiform fish. J. Comp. Neurol. *345:*224–252.

Maler, L., H.J. Karten, and M.V.L. Bennett (1973a) The central connections of the posterior lateral line nerve of *Gnathonemus petersii*. J. Comp. Neurol. *151:*57–66.

Maler, L., H.J. Karten, and M.V.L. Bennett (1973b) The central connections of the anterior lateral line nerve of *Gnathonemus petersii*. J. Comp. Neurol. *151:*67–84.

Maler, L., E. Sas, and J. Rogers (1981) The cytology of the posterior lateral line lobe of high-frequency weakly electric fish (Gymnotidae): Specificity in a simple cortex. J. Comp. Neurol. *195:*87–139.

Maler, L., E. Sas, C.E. Carr, and J. Matsubara (1982) Efferent projections of the posterior lateral line lobe in Gymnotiform fish. J. Comp. Neurol. *211:*154–164.

Mathieson, W.B., W. Heiligenberg, and L. Maler (1987) Ultrastructural studies of physiologically identified electrosensory afferent synapses in the Gymnotiform fish: *Eigenmannia*. J. Comp. Neurol. *255:*526–537.

McCormick, C.A. (1982) The organization of the octavolateralis area in actinopterygian fishes: A new interpretation. J. Morphol. *171:*159–181.

McCormick, C.A. (1983) Central connections of the octavolateralis nerves in the pike cichlid, Crenicichla lepidota. Brain Res. *263:*177–185.

Meek, J. (1981) A Golgi-electron microscopic study of goldfish optic tectum. I. Description of afferents, cell types and synapses. J. Comp. Neurol. *199:*149–173.

Meek, J. (1983) Functional anatomy of the tectum mesencephali of the goldfish. An explorative analysis of the functional implications of the laminar structural organization of the tectum. Brain Res. Rev. *6:*247–297.

Meek, J. (1992a) Why run parallel fibers parallel? Teleostean Purkinje cells as possible coincidence detectors in a timing device subserving spatial coding of temporal differences. Neuroscience *48:*249–283.

Meek, J. (1992b) Comparative aspects of cerebellar organization. From mormyrids to mammals. Eur. J. Morphol. *30:*37–51.

Meek, J. (1993) Structural organization of the mormyrid electrosensory lateral line lobe. J. Comp. Physiol. A *173:*675–677.

Meek, J. (1994) Microcircuitry of the mormyrid electrosensory lateral line lobe. Eur. J. Morphol. *32:*279–282.

Meek, J., and K. Grant (1994) The role of motor command feedback in electrosensory processing. Eur. J. Morphol. *32:*225–234.

Meek, J., and H.W.J. Joosten (1989) The distribution of serotonin in the brain of the mormyrid teleost *Gnathonemus petersii*. J. Comp. Neurol. *281:*206–224.

Meek, J., and R. Nieuwenhuys (1991) Palisade pattern of mormyrid Purkinje cells. A correlated light and electron microscopic study. J. Comp. Neurol. *306:*156–192.

Meek, J., R. Nieuwenhuys, and D. Elsevier (1986a) Afferent and efferent connections of the cerebellar lobe C_1 of the mormyrid fish *Gnathonemus petersii*: An HRP study. J. Comp. Neurol. *245:*319–341.

Meek, J., R. Nieuwenhuys, and D. Elsevier (1986b) Afferent and efferent connections of cerebellar lobe C3 of the mormyrid fish *Gnathonemus petersii*: An HRP study. J. Comp. Neurol. *245:*342–358.

Meek, J., T.G.M. Hafmans, L. Maler, and R. Hawkes (1992) The distribution of zebrin II in the gigantocerebellum of the mormyrid fish *Gnathonemus petersii* compared with other teleosts. J. Comp. Neurol. *316:*17–31.

Meek, J., H.W.J. Joosten, and T.G.M. Hafmans (1993) Distribution of noradrenaline-immunoreactivity in the brain of the mormyrid teleost *Gnathonemus petersii*. J. Comp. Neurol. *328:*145–160.

Meek, J., K. Grant, and T.G.M. Hafmans (1994) Multipolar intrazonal neurons in the mormyrid electrosensory lateral line lobe: Myelinated dendrites and reciprocal synaptic connections involved in center surround inhibition. Soc. Neurosci. Abstr. *20:*579.8.

Meek, J., K. Grant, Y. Sugawara, T. Hafmans, M. Veron, and J.P. Denizot (1996) Interneurons of the ganglionic layer in the mormyrid electrosensory lateral line lobe: Morphology, immunohistochemistry and synaptology. J. Comp. Neurol., this issue.

Meredith, G.E. (1984) Peripheral configuration and central projections of the lateral line system in *Astronotus ocellatus* (Cichlidae): A nonelectroreceptive teleost. J. Comp. Neurol. *288:*342–358.

Metz, C.B., S.P. Schneider, and R.E.W. Fyffe (1989) Selective suppression of endogenous peroxidase activity: Application for enhancing appearance of HRP-labeled neurons in vitro. J. Neurosci. Methods *26:*181–188.

Mugnaini, E., and L. Maler (1987) Cytology and immunocytochemistry of the nucleus of the lateral line lobe in the electric fish *Gnathonemus petersii* (Mormyridae): Evidence suggesting that GABAergic synapses mediate inhibitory corollary discharge. Synapse *1:*32–56.

Müller, M., T. Marti, and S. Kriz (1980) Improved structural preservation by freeze substitution. Elect. Microsc. *2:*720–721.

Nieuwenhuys, R., and C. Nicholson (1969) Aspects of the histology of the cerebellum of Mormyrid fishes. In R. Llinás (ed): Neurobiology of Cerebellar Evolution and Development. Chicago: AMA Education and Research Foundation, pp. 135–169.

Nieuwenhuys, R., E. Pouwels, and E. Smulders-Kersten (1974) The neuronal organization of cerebellar lobe C1 in the mormyrid fish *Gnathonemus petersii* (Teleostei). Z. Anat. Entwickl-Gesch. *144:*315–336.

Oertel, W.H., D.E. Schmechel, M.L. Tappaz, and I.J. Kopin (1981a) Production of a specific antiserum to rat brain glutamic acid decarboxylase by injection of an antigen-antibody complex. Neuroscience *6:*2689–2700.

Oertel, W.H., D.E. Schmechel, V.K. Weise, D.H. Ransom, M.L. Tappaz, H.C. Krutzsch, and I.J. Kopin (1981b) Comparison of cystein sulphinic acid carboxylase isoenzymes and glutamic acid decarboxylase in rat liver and brain. Neuroscience *6:*2701–2714.

Pouwels, E. (1978a) On the development of the cerebellum of the trout, *Salmo gairdneri*. III. Development of neuronal elements. Anat. Embryol. *153:*37–54.

Pouwels, E. (1978b) On the development of the cerebellum of the trout, *Salmo gairdneri*. IV. Development of the pattern of connectivity. Anat. Embryol. *153:*55–65.

Seguela, P., M. Geffard, R.M. Buijs, and M. le Moal (1984) Antibodies against γ-aminobutyric acid: Specificity studies and immunocytochemical results. Proc. Natl. Acad. Sci. USA *81:*3888–3892.

Smolen, A.J., L.L. Wright, and T.J. Cunningham (1983) Neuron numbers in the superior cervical sympathetic ganglion of the rat: A critical comparison of methods for cell counting. J. Neurocytol. *12:*739–750.

Szabo, T., M. Ravaille, S. Libouban, and P.S. Enger (1983) The mormyrid rhombencephalon. I. Light and EM investigations on the structure and connections of the lateral line lobe nucleus with HRP labeling. Brain Res. *266:*1–19.

van den Pol, A.N., and T. Görcs (1986) Synaptic relationships between neurons containing vasopressin, gastrin-releasing peptide, vasoactive intestinal polypeptide, and glutamate decarboxylase immunoreactivity in the suprachiasmatic nucleus: Dual ultrastructural immunocytochemistry with gold-substituted silver peroxidase. J. Comp. Neurol. *252:*507–521.

Wang, D., and L. Maler (1994) The immunocytochemical localization of glutamate in the electrosensory system of the gymnotiform fish, *Apteronotus leptorhynchus*. Brain Res. *653:*215–222.

Wolf, K. (1963) Physiological salines for freshwater teleosts. Progr. Fish Culturist *25:*135–140.

Zakon, H.H. (1986) The electroreceptive perifery. In T.H. Bullock and W. Heiligenberg (eds): Electroreception. New York: John Wiley and Sons, pp. 103–156.

Zupanc, G.K.H., and I. Horschke (1995) Proliferation zones in the brain of adult gymnotiform fish: A quantitative mapping study. J. Comp. Neurol. *353:*213–233.